Differentiation-defective phenotypes revealed by large-scale analyses of human pluripotent stem cells.

AUTHOR(S):

Koyanagi-Aoi, Michiyo; Ohnuki, Mari; Takahashi, Kazutoshi; Okita, Keisuke; Noma, Hisashi; Sawamura, Yuka; Teramoto, Ito; ... Sato, Tosiya; Takahashi, Jun; Yamanaka, Shinya

CITATION:

Koyanagi-Aoi, Michiyo ...[et al]. Differentiation-defective phenotypes revealed by large-scale analyses of human pluripotent stem cells.. Proceedings of the National Academy of Sciences of the United States of America 2013, 110(51): 20569-20574

ISSUE DATE:

2013-11-20

URL:

http://hdl.handle.net/2433/179528

Title Page

***Classification*:** BIOLOGICAL SCIENCES/ Cell biology

***Title*:** Differentiation defective phenotypes revealed by large scale analyses of human pluripotent stem cells

Author affiliation: Michiyo Koyanagi-Aoi[a,1], Mari Ohnuki[a,1], Kazutoshi Takahashi[a], Keisuke Okita[a] , Hisashi Noma[b], Yuka Sawamura[a], Ito Teramoto[a], Megumi Narita[a], Yoshiko Sato[a], Tomoko Ichisaka[a], Naoki Amano[a], Akira Watanabe[a], Asuka Morizane[a], Yasuhiro Yamada[a,d], Tosiya Sato[e], Jun Takahashi[a,c] and Shinya Yamanaka[a,f,2]

[a] Center for iPS Cell Research and Application (CiRA), Kyoto University, Kyoto 606-8507, Japan

[b] Department of Data Science, The Institute of Statistical Mathematics, Tokyo 190-8562, Japan

[c] Department of Biological Repair, Institute for Frontier Medical Sciences, Kyoto University, Kyoto 606-8507, Japan

[d] Institute for Integrated Cell-Material Sciences (WPI-iCeMS), Kyoto University, Kyoto, 606-8507, Japan

[e] Department of Biostatistics, Kyoto University School of Public Health, Kyoto 606-8501, Japan

[f] Gladstone Institute of Cardiovascular Disease, San Francisco, California 94158, USA

[1] These authors contributed equally to this work

[2] To whom correspondence should be addressed

Corresponding author : Shinya Yamanaka, Center for iPS Cell Research and Application (CiRA), Kyoto University, Kyoto 606-8507, Japan, +81-075-366-7044, yamanaka@cira.kyoto-u.ac.jp

Abstract

We examined the gene expression and DNA methylation of 49 hiPSCs and 10 hESCs and found overlapped variations in gene expression and DNA methylation in the two types of human pluripotent stem cell lines. Comparisons of the *in vitro* neural differentiation of 40 hiPSCs and 10 hESCs showed that seven hiPSC clones retained a significant number of undifferentiated cells even after neural differentiation culture, and formed teratoma when transplanted into mouse brains. These differentiation-defective hiPSC clones were marked by higher expression levels of several genes, including those expressed from long terminal repeats of specific human endogenous retroviruses. These data demonstrated a subset of hiPSC lines that have aberrant gene expression and defective potential in neural differentiation, which need to be identified and eliminated prior to applications in regenerative medicine.

Significance statement

In the past few years, the findings have been controversial in regard to whether human induced pluripotent stem cells (hiPSCs) are distinct from human embryonic stem cells (hESCs) in their molecular signatures and differentiation properties. In this study, hiPSCs and hESCs have overlapping variations in molecular signatures such as RNA expression and DNA methylation. On the other hand, some hiPSC clones retained a significant number of undifferentiated cells even after neural differentiation culture, and formed teratoma when transplanted into mouse brains. These differentiation-defective hiPSC clones were marked by higher expression levels of several genes, including those expressed from long terminal repeats of specific human endogenous retroviruses. They need to be identified and eliminated prior to applications in regenerative medicine.

INTRODUCTION

Human pluripotent stem cells possess a robust potential for proliferation and provide useful sources of cells for regenerative medicine and drug discovery. Two types of human pluripotent stem cells have been generated: human embryonic stem cells (hESCs) derived from blastocysts (1), and induced pluripotent stem cells (hiPSCs), which are generated from somatic cells by factor-mediated reprogramming (2, 3).

In the past few years, the findings have been controversial in regard to whether hESCs and hiPSCs are distinct cell types. Some reports have argued that they could not be clearly distinguished (4-6), whereas others have reported that they have differences in their gene expression (7-10), DNA methylation (10-13), and capacity for differentiation (14). In the latter papers, relatively small numbers of cell lines were generally compared. In addition, most comparisons used pluripotent cell lines from various laboratories, such that the observed differences may be attributable to lab-specific variations due to technical differences (15).

To overcome these problems, we compared the mRNA and microRNA (miRNA) expression levels and DNA methylation between 10 hESCs and 49 hiPSCs that had been cultured under the same conditions. Furthermore, we compared the *in vitro* directed neural differentiation of these pluripotent stem cells.

RESULTS

Overlapped variations of the mRNA expression and DNA methylation in hiPSCs and hESCs

We analyzed a total of 49 hiPSCs derived from four types of somatic cells, including human dermal fibroblasts (HDFs), dental-pulp stem cells (DP), cord blood cells (CB) and peripheral blood mononuclear cells (PBMN), generated using three gene delivery methods, including those employing retroviruses, non-integration episomal plasmids and Sendai viruses (**Table 1 and Dataset S1)**. Most clones were generated in our own laboratory, except for three clones that were established in another laboratory (16). Prior to the analyses of the gene/miRNA expression (**Figs. 1A, B)** and DNA methylation **(Fig. 1C)**, we cultured these hiPSCs, as well as 10 hESCs, under the same culture conditions for at least three passages. In addition, we analyzed the original somatic cells, two human embryonic carcinoma cell (ECC) lines (NTera2 cloneD1 and 2102Ep 4D3) and three cancer cell lines (HepG2, MCF7 and Jurkat).

The mRNA microarray analyses (**Fig. 1A**) identified 61 probes with significant differences in expression between hESCs and hiPSCs (*t*-test: FDR<0.05). Each of the 61 probes showed variable expression among both the hESCs and hiPSCs, and the distributions of the expression levels in the two groups overlapped (**Fig. 1D**). Of note,

hESCs established at Kyoto University (Kyoto hESCs) were more similar to hiPSCs than to the remaining hESCs (other hESCs) in their expression of 15 probes, that were differentially expressed between hESCs and hiPSCs (FDR < 0.05 and FC > 3) (**Fig. S1A**). In contrast, hierarchical clustering using all probes showed no clear cut separation among Kyoto hESCs, other ESCs, and iPSCs, indicating that the similarity of Kyoto ESCs to iPSCs are confined to a small set of genes (**Fig. S1B)**. In addition, the miRNA array analyses (**Fig. 1B**) did not find any significant differences between hESCs and hiPSCs (*t*-test: FDR<0.05). The expressions of hsa-miR-886-3p and hsa-miR-142-3p tended to be higher in hiPSCs, but the expression levels of these miRNAs showed overlapped variations among hiPSCs and hESCs (**Fig. S1A**).

We next compared the global DNA methylation status between hiPSCs and hESCs by the Illumina Infinium Human Methylation27 BeadChip assay. Among 27,445 CpG dinucleotides examined, we did not identify significantly differentially methylated CpG regions (CG-DMR) between the hESCs and hiPSCs (Mann-Whitney's U test, FDR<0.05) (**Fig. 1C**).

We then validated the CG-DMRs reported in previous studies. Three studies identified a total of 205 regions as CG-DMRs, including 130, 71 and four regions identified by comparing five hiPSCs and two hESCs (13), three versus three (12) and

nine versus three (10) cell lines, respectively. Of the 205 regions, 46 regions containing 66 CpG dinucleotides were covered by the Infinium platform used in our study (**Table S1A**). Based on the methylation levels in our hiPSCs and hESCs, these CpGs were clustered into three groups (**Fig. 1E**). Two-thirds of these CpGs belonged to group A: they tended to be highly methylated in hESCs, ECCs and cancer cell lines, whereas they tended to be hypomethylated in hiPSCs, as well as somatic cells. However, they were also hypomethylated in Kyoto ESCs (17). The methylation status of the upstream region of the *PON3* gene, a representative example of CpGs in a Group A, was confirmed by pyrosequencing (**Fig. 1F**). Thus, the CpG methylation status in Group A may distinguish some, but not all, hESCs from hiPSCs. Seventeen CpGs belonged to group B, which showed similar methylation levels in both hESCs and hiPSCs. Five CpGs, representing three genes, belonged to group C and showed higher methylation levels in some, but not all, hiPSCs compared to hESCs. The remaining hiPSCs showed low methylation levels, comparable to those in hESCs. We confirmed the methylation status of a representative example of CpGs in a group C, the upstream region of the *TCERG1L* gene, by pyrosequencing; the methylation levels were low in 21 of the 49 hiPSCs (**Fig. 1G**). Therefore, the CpGs in group C may distinguish some, but not all, iPSCs from hESCs.

A previous report (12) showed that many CG-DMRs were located in CpG shores, rather than CpG islands. Since only a few (9 out of 71) of their CG-DMRs were covered by our Infinium platform, we analyzed five CG-DMRs in CpG shores by pyrosequencing, including *A2BP1*, *IGF1R*, *POU3F4*, *PTPRT* and *ZNF184* (**Fig. S1C**). We detected significant differences in the averaged DNA methylation levels between hESCs and hiPSCs in four out of five genes. However, variations of DNA methylation levels in hESCs and hiPSCs are overlapped. They may distinguish some, but not all, hiPSCs from hESCs.

A subset of hiPSC clones retain undifferentiated cells after neural differentiation

To examine whether hESCs and hiPSCs have comparable differentiation potential, we performed *in vitro* directed differentiation into neural stem and progenitor cells using the modified serum-free floating culture of embryoid body-like aggregates (SFEBq) method (**Fig. 2A**) (18). We initially performed the neural induction of two hESCs and 21 hiPSCs. Fourteen days after induction, the differentiation efficiency was evaluated based on the expression of an early neural marker, polysialylated neural cell adhesion molecule (PSA-NCAM). We found that all hESCs and hiPSCs differentiated into PSA-NCAM^{+} cells with more than 80% efficiency (**Fig. 2B**). We also quantified the expression levels of the early neural marker, *PAX6*, and the late neural marker, *MAP2*, in

neurospheres by qRT-PCR (**Fig. S2A**). All the examined hES/iPSCsexpressed *PAX6* at >100-fold higher levels, and *MAP2* at >20-fold higher levels in comparison to undifferentiated H9 hESC. However, in some hiPSCs, we noticed slightly lower differentiation efficiency than the remaining hiPSCs and hESCs **(Fig. 2B**). This lower efficiency in neural differentiation was inversely correlated with a higher proportion of OCT3/4^{+} and TRA1-60^{+} undifferentiated cells (**Fig. 2C**). We also detected residual undifferentiated cells after a different neural differentiation protocol using adhesion culture (19) (**Fig. S2B**).

We then increased the number of clones and examined the proportions of OCT3/4^{+} undifferentiated cells after neural induction from 10 hESCs and 40 hiPSCs. The 50 clones were ranked according to their proportions of OCT3/4^{+} cells on day 14 (**Dataset S1** and **Fig. 2D**). The proportions of OCT3/4^{+} cells varied from 0% to ~20%. Thirty-eight clones, including nine hESCs and 29 hiPSCs, showed less than 1% OCT3/4^{+} cells in all experiments. We designated these clones as “good” clones. On the other hand, seven hiPSCs contained more than 10% OCT3/4^{+} cells after neural differentiation in at least one experiment. We designated these clones as “differentiation-defective” clones. Clones which were not “good” or “defective” were categorized as “intermediate”.

Activation of specific LTR7 elements in "differentiation-defective" clones

To identify molecular signatures that can predict "differentiation-defective" clones, we compared the global gene expression patterns of 38 "good" clones and seven "differentiation-defective" clones under the culture conditions used for the undifferentiated state. We identified 19 probes (13 putative transcripts) that showed > 5-fold differences in expression, with a FDR <0.05, shown by magenta dots in **Fig. 3A** and listed in **Table S1B**.

Of the 19 probes identified, five probes recognized *HHLA1* (human endogenous retrovirus-H LTR–associating 1). Previous reports have shown that *HHLA1* is regulated by a long terminal repeat (LTR) of a human endogenous retrovirus-H (HERV-H) (20). The LTR in *HHLA1* is classified as LTR7. Moreover, among the genes recognized by the 19 probes, we found that at least two others, *ABHD12B* and *C4orf51*, also contained LTR7 sequences in their gene bodies. According to a microarray analysis, we confirmed that these three LTR7-containing genes were upregulated in the "differentiation-defective" hiPSCs, as well as the nullipotent hECC line 2102Ep 4D3(21), but they were expressed at lower levels in the "good" hiPSCs, hESCs, pluripotent hECC line NTera2 cloneD1, while they were almost not expressed in the

original somatic cells (**Fig. 3B**).

The Agilent microarray platform has 12 probes, including two reverse probes [d(r), f(r)], for *HHLA1* and its neighboring gene, *OC90*, which is reported to make a fusion transcript with HHLA1 (20) (**Fig. 3C**). Among them, seven probes located downstream of LTR7 showed higher expression levels in "differentiation-defective" clones than in "good" clones (**Figs. 3C, D**). Similarly, there are two probes for *ABHD12B*, designed for exons 4 and 13 (**Fig. 3C)**. Only the exon 13 probe, located downstream of LTR7, showed a higher expression in "differentiation-defective" clones than in "good" clones (**Fig. 3D**). We also performed an exon array (Affymetrix) of *ABHD12B* and *C4orf51*, and found that exons downstream of LTR7 were preferentially upregulated in "differentiation-defective" hiPSC clones (**Fig. 3E**). We also found that the methylation status of LTR7s in these three genes were lower in "differentiation-defective" hiPSC clones than in "good" clones (**Fig. 3F**). These results indicate that the three genes are transcribed from activated LTR7.

DNA hypomethylation exists in some, but not all, of LTR7s in "differentiation-defective" clones

According to the Repeatmasker software program, there are 3523 LTR7 elements in

the human genome. In order to extract microarray probes that are potentially affected by LTR7s, we first selected genes containing LTR7s in their gene bodies or regions 2 kb upstream from their transcription start sites. We then retrieved the microarray probes located between each LTR7 and the 3' end of the corresponding gene body. As a result, we selected 763 probes as LTR7-related probes (**Fig. S3A and Table S1C**). We found that most of these probes showed comparable expression levels in "good" and "defective" lines (**Fig. S3B**), with the exception of some probes, such as those corresponding to *ARRB1*, *FAAH2* and *TBC1D23*, that were differentially expressed between "good" and "defective" clones (FDR < 0.05 and FC >2) and showed slightly higher expression in "defective" lines.

We then checked the DNA methylation status of the LTR7 regions in these three genes and three other genes (*DNMT3B*, *ABCA1* and *APP*) whose expression levels were not significantly different between the "good" and "defective" clones. By pyrosequencing and clonal bisulfite sequencing, we found that the LTR7 regions in four genes (*ARRB1*, *FAAH2*, *TBC1D23* and *APP*) were hypomethylated in "defective" clones compared to "good" clones. In contrast, the LTR7 regions in two genes (*DNMT3B* and *ABCA1*) did not show such hypomethylation (**Fig. S3C**). Therefore, the activation of LTR7 is not confined to *HHLA1*, *ABHD12B* and *C4orf51*; DNA hypomethylation exists in some, but

not all, of LTR7s in “defective” hiPSCs.

“Differentiation-defective” hiPSC clones form teratomas in mouse brains

To further evaluate the “defective” hiPSCs, we induced their differentiation into dopaminergic neurons, which were then transplanted into the striata of nonobese diabetic/severe combined immune deficient (NOD/SCID) mouse brains (**Fig. 4A**). Thirty and sixty days after transplantation, we obtained T2-weighted images of the mouse brains with a magnetic resonance imaging (MRI) scanner to observe the graft sizes at the transplanted sites (**Fig. 4B**). The quantification of the MR images showed that “defective” hiPSC clones resulted in significantly larger graft sizes than “good” clones (**Fig. 4C**). Notably, some mice that had received “defective” clones died or developed symptoms that required euthanasia before day 60 (**Table S2**). Therefore, we could not obtain the graft size data on day 60 in these mice.

To identify the composition of the surviving grafts, we performed a histological analysis of the brains of animals that died or that became moribund after transplantation. The remaining healthy mice were sacrificed 14–41 weeks after transplantation. Sections were stained with hematoxylin and eosin (HE). Thirty-six out of the 42 grafts (85.7%) from “defective” clones contained non-neural lineage tissues, such as intestine-like

epithelial cells, cartilage or mesenchymal cells (**Fig. 4D** and **Fig. S4A**). In contrast, grafts from "good" clones largely consisted of neural tissues. Immunostaining confirmed grafts were positive for human NCAM (**Fig. S4B**). A qRT-PCR analysis of pre-transplanted cells from "defective" clones revealed higher expression levels of OCT3/4, suggesting that some undifferentiated cells still remained even after 29 days neural induction (**Fig. 4E**). We then depleted the TRA-1-60^{+} cells on day 22 during neural induction, and transplanted cells on day 29. The TRA-1-60-depleted cells from "defective" clones resulted in significantly smaller grafts, which did not contain non-neural tissues (**Fig. S4C**).

We also observed that 14 out of the 63 (22.2%) grafts from "good" clones, including those from hESCs, contained a non-neural component in the graft tissue after transplantation (**Fig. 4D and Table S2),** although these clones did not show high expression levels of OCT3/4 in the pre-transplantation samples (**Fig. 4E**). We referred to these clones as "type 2 defective" clones, which were distinct from "type 1 defective" clones that contained *OCT3/4*$^{+}$ undifferentiated cells in the pre-transplantation samples. We observed higher expression levels of *SOX17* (an endoderm marker) and *GSC* (an endoderm and mesoderm marker) in the pre-transplantation samples of "type 2 defective" clones (**Figs. 4F, G**), demonstrating the presence of other lineages in these

pre-transplantation samples.

Discussion

We identified two types of "defective" pluripotent stem cell lines in this study. The first type consisted of hiPSCs that retained a substantial number of undifferentiated cells after *in vitro* directed neural differentiation. Seven out of the 40 iPSCs (17.5%) examined in this study fell into this category. In contrast, we did not observe such defects in any of the 10 hESCs. More clones should be analyzed to confirm that hESCs are free from this deficiency. Nevertheless, it is likely that "type 1 defectiveness" is more common in hiPSCs than in hESCs. The "type 1 defective" hiPSCs are accompanied by an aberrant epigenetic status. Among the 13 putative transcripts that were highly expressed in these defective clones, at least three were expressed from the LTR of endogenous retroviruses. Normally, these LTRs are silenced by various epigenetic modifications, including DNA methylation (22-24). In "type 1 -defective" iPSC clones, LTR locus in the three genes showed lower DNA methylation levels than in "good" clones and original somatic cells. Notably, the same regions were hypo-methylated in the nullipotent hECC line, 2102Ep 4D3, suggesting that the loss of DNA methylation in these LTR locus is correlated with the lower ability to differentiate. At present, the biological significance and relationship between activation of specific

LTRs and the defective phenotype is unclear. Recent reports showed that ERV may play roles in the establishment and maintenance of transcription network in pluripotent stem cells (25, 26). Furthermore, updated annotations revealed that one of differentially expressed probes in "type 1 defective" hiPSCs (A_19_P00325604) encoded *large intergenic non-coding RNA regulator of reprogramming (Linc-ROR)*, which contained LTR7 in its 5' region. *Linc-ROR* is reported to have multiple roles in the induction and maintenance of pluripotency (27, 28). Future studies should be undertaken to clarify why these epigenetic abnormalities occur and how they are related to the defective differentiation.

Kim et al. (29) showed that there is an inverse correlation between the hsa-mir-371-373 expression and the efficiency of neural differentiation. They also showed that KLF4 may induce the expression of hsa-mir-371-373. In our analyses, the hsa-mir-371-373 cluster was highly expressed in all the seven "type 1 defective" hiPSC clones (**Fig. S5A**). However, the cluster was also highly expressed in many "good" clones. KLF4 was highly expressed in some "defective" clones (**Fig. S5B**), and four out of six retroviral "defective" clones failed to silence KLF4 retroviral transgenes (**Fig. S5C**). There was no correlation between the OCT3/4 transgene expression and "type 1 defectiveness" (**Fig. S5D**). Taken together, these findings indicate that high expression

levels of the hsa-mir-371-373 cluster, KLF4 and transgenes cannot function as absolute markers for “type 1 defectiveness”.

We previously reported that the origin of mouse iPSCs was a major determinant of defectiveness in directed neural differentiation; mouse iPSCs from adult tail tip fibroblasts showed the highest incidence of resistance to differentiation (30). In the present study using human iPSCs, five out of seven “type 1 -defective” clones were derived from fibroblasts of donors of various ages, and six out of the seven clones were generated using retroviruses (**Table 1**). This may suggest that “type 1 defectiveness” is associated with fibroblast origin and retroviral induction. However in this study, most of the fibroblast-derived iPSCs were generated by retroviruses, and most of the non-fibroblast iPSCs were generated by non-retroviral methods. Future studies will need to be undertaken to determine whether the origin or the generation method (or both) has a significant impact on the frequency of “type 1 differentiation-defective” iPSCs.

The second type of “defective” group includes hiPSCs and hESCs that contained differentiated cells of non-neural lineages after *in vitro* directed differentiation into dopaminergic neurons. We have previously shown that the optimal conditions for hepatic differentiation are different for each clone (16). By optimizing the protocols, it

may be possible to induce complete neural differentiation to avoid “type 2 defective” clones. Alternatively, purification of neural cells using a cell sorter may work to avert “type 2 defective” clones.

Several studies have reported sets of genes of which DNA methylation status are different between hiPSCs and hESCs. We validated these CG-DMRs and found that many of them can distinguish some hESCs from hiPSCs (Group A in **Fig. 1E**). They are highly methylated in some hESCs, but not in hiPSCs or original somatic cells. Thus these CG-DMRs may represent epigenetic memories of somatic cells in iPSCs. However, we found a set of hESCs that showed low methylation status of these CG-DMRs, which were comparable to hiPSCs. We also found another set of the reported CG-DMRs that showed high methylation status in some hiPSCs, but not in original somatic cells or hESCs (Group C in **Fig. 1E**). These likely represent aberrant methylation associated with reprogramming. However, we also found many hiPSCs showed normal methylation patters of these CG-DMRs. A more recent study identified nine genes that can segregate hiPSCs from hESCs in DNA methylation and gene expression (31). However, we did not observe such a clear distinction in gene expression of these genes between our hiPSCs and hESCs (**Fig. S6)**. Two of these genes, *TCERG1L* and *FAM19A5* may distinguish some, but not all, hiPSCs from hESCs.

In our analyses, 35 hiPSCs had records of the donor's genetic background; 14 were derived from Caucasians and 21 were from Japanese subjects (**Dataset S1**). Thus, the similarity of some signatures between the Kyoto hESCs and our hiPSCs cannot be attributed to the racial or ethnic backgrounds of the donors. Another possible cause of the differences is the method used to establish the hESCs and the subsequent culture conditions. The Kyoto hESCs were generated on feeders consisting of a 1:1 mixture of MEFs and SL10 cells (17, 32), which were subcloned from STO cells. Most of our hiPSCs were established on SNL feeders, which were also derived from STO cells. A recent report showed that the feeders have profound effects on established hiPSCs (33). To confirm the importance of the culture conditions, more studies comparing hESC/hiPSCs established under different conditions will be needed.

In conclusion, our results revealed that a subset of hiPSCs is defective in neural differentiation and marked with activation of endogenous retroviruses. We also confirmed that some hiPSCs are different from hESCs in molecular signatures, including CG-DMRs that have been previously reported. It remained to be determined whether these molecular signatures specific for some hiPSCs have functional consequences.

Materials and Methods

The gene expression profiling was carried out using the SurePrint G3 human GE microarray (Agilent). Most of the data were analyzed using the Gene spring GX 11.5.1 software program (Agilent Technologies). Neural induction was performed as described previously (18). Detailed descriptions of methods in this article are available in SI Materials and Methods.

ACKNOWLEDGMENTS

We thank Drs. Takashi Aoi, Yoshinori Yoshida, Masato Nakagawa and other members of the Yamanaka research group for their valuable scientific discussions; Drs. Takuya Yamamoto, Toshiki Taya and Tomoaki Tsubota for giving advice about bioinformatics; Dr. Hirofumi Suemori for hES cell lines; Drs. Koji Eto and Naoya Takayama for TKCB hiPS cell lines; Akiko Otsuka for RNA and genomic DNA samples; Dr. Takafumi Kimura and Takaomi Futakami for HLA analysis and Aki Sasaki, Tomomi Ito, Midori

Yokura, Ayumi Ichikawa for technical assistance. We also thank Naoki Nagata, Yoko Miyake, Rie Kato, Eri Minamitani, Sayaka Takeshima and Ryoko Fujiwara for their valuable administrative support. This work was supported in part by Grants-in-Aid for Scientific Research from the Japanese Society for the Promotion of Science; from the Ministry of Education, Culture, Sports, Science, and Technology; by a grant from the Leading Project of the Ministry of Education, Culture, Sports, Science, and Technology and by a grant from the Funding Program for World-Leading Innovative Research and Development on Science and Technology (First Program) of the Japanese Society for the Promotion of Science. M.K. and M.O. were Research Fellows of the Japanese Society for the Promotion of Science.

References

1. Thomson JA, *et al.* (1998) Embryonic stem cell lines derived from human blastocysts. *Science* 282(5391):1145-1147.
2. Takahashi K, *et al.* (2007) Induction of pluripotent stem cells from adult human fibroblasts by defined factors. *Cell* 131(5):861-872.
3. Yu J, *et al.* (2007) Induced pluripotent stem cell lines derived from human somatic cells. *Science* 318(5858):1917-1920.
4. Bock C, *et al.* (2011) Reference Maps of human ES and iPS cell variation enable high-throughput characterization of pluripotent cell lines. *Cell* 144(3):439-452.
5. Newman AM & Cooper JB (2010) Lab-Specific Gene Expression Signatures in Pluripotent Stem Cells. *Cell Stem Cell* 7(2):258-262.
6. Guenther MG, *et al.* (2010) Chromatin structure and gene expression programs of human embryonic and induced pluripotent stem cells. *Cell Stem Cell* 7(2):249-257.

7. Chin MH, *et al.* (2009) Induced pluripotent stem cells and embryonic stem cells are distinguished by gene expression signatures. *Cell Stem Cell* 5(1):111-123.
8. Marchetto MC, *et al.* (2009) Transcriptional signature and memory retention of human-induced pluripotent stem cells. *PLoS ONE* 4(9):e7076.
9. Ghosh Z, *et al.* (2010) Persistent donor cell gene expression among human induced pluripotent stem cells contributes to differences with human embryonic stem cells. *PLoS ONE* 5(2):e8975.
10. Ohi Y, *et al.* (2011) Incomplete DNA methylation underlies a transcriptional memory of somatic cells in human iPS cells. *Nat Cell Biol* 13(5):541-549.
11. Deng J, *et al.* (2009) Targeted bisulfite sequencing reveals changes in DNA methylation associated with nuclear reprogramming. *Nat Biotechnol* 27(4):353-360.
12. Doi A, *et al.* (2009) Differential methylation of tissue- and cancer-specific CpG island shores distinguishes human induced pluripotent stem cells, embryonic stem cells and fibroblasts. *Nat Genet* 41(12):1350-1353.
13. Lister R, *et al.* (2011) Hotspots of aberrant epigenomic reprogramming in human induced pluripotent stem cells. *Nature* 471(7336):68-73.
14. Hu BY, *et al.* (2010) Neural differentiation of human induced pluripotent stem cells follows developmental principles but with variable potency. *Proc Natl Acad Sci U S A* 107(9):4335-4340.
15. Yamanaka S (2012) Induced pluripotent stem cells: past, present, and future. *Cell Stem Cell* 10(6):678-684.
16. Kajiwara M, *et al.* (2012) Donor-dependent variations in hepatic differentiation from human-induced pluripotent stem cells. *Proc Natl Acad Sci U S A* 109(31):12538-12543.
17. Suemori H, *et al.* (2006) Efficient establishment of human embryonic stem cell lines and long-term maintenance with stable karyotype by enzymatic bulk passage. *Biochem Biophys Res Commun* 345(3):926-932.
18. Morizane A, Doi D, Kikuchi T, Nishimura K, & Takahashi J (2011) Small-molecule inhibitors of bone morphogenic protein and activin/nodal signals promote highly efficient neural induction from human pluripotent stem cells. *J Neurosci Res* 89(2):117-126.
19. Kriks S, *et al.* (2011) Dopamine neurons derived from human ES cells efficiently engraft in animal models of Parkinson's disease. *Nature* 480(7378):547-551.
20. Kowalski PE, Freeman JD, & Mager DL (1999) Intergenic splicing between a HERV-H endogenous retrovirus and two adjacent human genes. *Genomics* 57(3):371-379.

21. Bahrami AR, Matin MM, & Andrews PW (2005) The CDK inhibitor p27 enhances neural differentiation in pluripotent NTERA2 human EC cells, but does not permit differentiation of 2102Ep nullipotent human EC cells. *Mech Dev* 122(9):1034-1042.
22. Rowe HM & Trono D (2011) Dynamic control of endogenous retroviruses during development. *Virology* 411(2):273-287.
23. Hutnick LK, Huang X, Loo TC, Ma Z, & Fan G (2010) Repression of retrotransposal elements in mouse embryonic stem cells is primarily mediated by a DNA methylation-independent mechanism. *J Biol Chem* 285(27):21082-21091.
24. Stoye JP (2012) Studies of endogenous retroviruses reveal a continuing evolutionary saga. *Nat Rev Microbiol* 10(6):395-406.
25. Macfarlan TS, *et al.* (2012) Embryonic stem cell potency fluctuates with endogenous retrovirus activity. *Nature* 487(7405):57-63.
26. Santoni FA, Guerra J, & Luban J (2012) HERV-H RNA is abundant in human embryonic stem cells and a precise marker for pluripotency. *Retrovirology* 9:111.
27. Loewer S, *et al.* (2010) Large intergenic non-coding RNA-RoR modulates reprogramming of human induced pluripotent stem cells. *Nat Genet* 42(12):1113-1117.
28. Wang Y, *et al.* (2013) Endogenous miRNA sponge lincRNA-RoR regulates Oct4, Nanog, and Sox2 in human embryonic stem cell self-renewal. *Dev Cell* 25(1):69-80.
29. Kim H, *et al.* (2011) miR-371-3 expression predicts neural differentiation propensity in human pluripotent stem cells. *Cell Stem Cell* 8(6):695-706.
30. Miura K, *et al.* (2009) Variation in the safety of induced pluripotent stem cell lines. *Nat Biotechnol* 27(8):743-745.
31. Ruiz S, *et al.* (2012) Identification of a specific reprogramming-associated epigenetic signature in human induced pluripotent stem cells. *Proc Natl Acad Sci U S A* 109(40):16196-16201.
32. Kawase E, *et al.* (1994) Strain difference in establishment of mouse embryonic stem (ES) cell lines. *Int J Dev Biol* 38(2):385-390.
33. Tomoda K, *et al.* (2012) Derivation conditions impact x-inactivation status in female human induced pluripotent stem cells. *Cell Stem Cell* 11(1):91-99.

FIGURE LEGENDS

Fig. 1. hiPSCs and hESCs have overlapped variations in RNA expression and DNA

methylation

(A)-(C) Scatter plots of the mRNA expression (**A**), miRNA expression (**B**) and DNA methylation **(C)** data comparing the average of 49 hiPSC lines (y-axis) to the average of 10 hESC lines (x-axis) are shown. The RNA expression value is shown on a log 2 scale. Green lines indicate two-fold differences in the RNA expression levels between the clones. Differentially expressed probes (*t*-test, FDR<0.05) are shown in magenta. (**D**) The variations in the mRNA expression levels of 61 differentially expressed probes in hESCs (red) and hiPSCs (black) are shown. Probes are arranged in order of the absolute value of the fold change (FC) between hESCs and hiPSCs. (**E**) The DNA methylation profiles for CpGs contained in reported hES-hiPS DMRs and overlapping with our platform. Probes are arranged in order of the differences between the average DNA methylation level of hESCs and that of hiPSCs. The heat map represents the DNA methylation levels from completely methylated (= 1, magenta) to unmethylated (= 0, white) samples. (**F**)(**G**) The methylation status of the upstream region of *PON3* (**F**) and *TCERG1L* (**G**) was examined by pyrosequencing.

Fig. 2. A differentiation-defective phenotype in a subset of hiPSC clones. (A) A schematic diagram of the SFEBq method used for neural differentiation. (B) Neural

induction was performed for two hESC and 21 hiPSC lines which were established from various origins by retroviral or episomal vector methods. On day 14, we examined the proportion of PSA-NCAM-expressing cells by flow cytometry (n = 2). (C) The proportions of PSA-NCAM- (white), OCT3/4- (grey) and TRA1-60- (black) positive cells 14 days after neural differentiation. (D) The proportions of $OCT3/4^{+}$ cells on day 14 after neural differentiation are ranked in order of their maximum value. The numbers in parentheses show the number of trials.

Fig. 3 Activation of specific endogenous retroviral LTR7s in "defective" clones

(A) A scatter plot of the mRNA expression data comparing the average of 38 "good" clones (y-axis) to the average of seven "defective" clones (x-axis). Green lines indicate five-fold differences in expression. A total of 19 differentially expressed probes are colored magenta. (B) The expression levels of LTR7-related genes (*HHLA1, ABHD12B* and *C4orf51*) were examined by microarray. (C) A schematic diagram of three LTR7-related genes. *HHLA1* and *OC90* are neighboring genes. Dots indicate microarray probes. Magenta dots show probes which are located after LTR7 regions, which were upregulated in "defective" clones. (D) A scatter plot of array probes which recognized LTR7-related genes and two other genes (*EFR3A* and *KCNQ3*) which are genes

neighboring *HHLA1* and *OC90*, respectively. (E) The exon array of the *ABHD12B* and *C4orf51* genes. The average levels of the normalized exon expression are shown. (F) The DNA methylation status of LTR7 and its neighboring regions of *HHLA1*, *ABHD12B* and *C4orf51* was examined by pyrosequencing**.** (n.s.; not significant, *; $p<0.05$, **; $p<0.01$, Mann-Whitney's U-test)

Fig. 4 Transplantation of neural cells derived from hiPSCs and hESCs into mouse brains

(A) A schematic diagram of the SFEBq method used for DA neural differentiation. On day 29, the cells were transplanted into NOD/SCID mouse brains. (B) Magnetic resonance images of coronal sections of the grafted brains. The section surface of grafted cells indicated as the white shadow in right brain was measured as described in the lower panels. (C) A box-and-whisker plot of the surface sizes of graft sections 30 and 60 days after transplantation. The median, quartile and range are shown. *t-test, $p<0.05$. (D) The proportion of each kind of graft. Grafts were categorized according to their components as determined in HE sections, and were classified by the proportion of neural tissues by a microscopic observation. (E)-(G) The expression levels of the undifferentiated cell marker, *OCT3/4* (E), the endoderm marker, *SOX17* (F), and the

mesoderm and endoderm marker, *GSC* (G), in pre-transplantation cultures, undifferentiated hESC lines and somatic cells (HDF and DP) were examined by qRT-PCR. The colors of the dots were identical to the proportion of neural tissues in **Fig. 4D**.

Table 1. A summary of the iPSC clones used in this report

		Method used to generate clones			
		Retrovirus	Episomal plasmid	Sendaivirus	Total
Origin	HDFs	22 (5,0)	3 (0,0)	0 (0,0)	25 (5,0)
	DP cells	1 (0,0)	2 (1,1)	0 (0,0)	3 (1,1)
	CB	3 (1,2)	4 (0,0)	5 (0,0)	12 (1,2)
	PBMN	0 (0,0)	5 (0,1)	4 (0,0)	9 (0,1)
	Total	26 (6,2)	14 (1,2)	9 (0,0)	49 (7,4)

Total clone numbers with “type 1 defective” clone number and “type 2 defective” clone number in parentheses are shown.

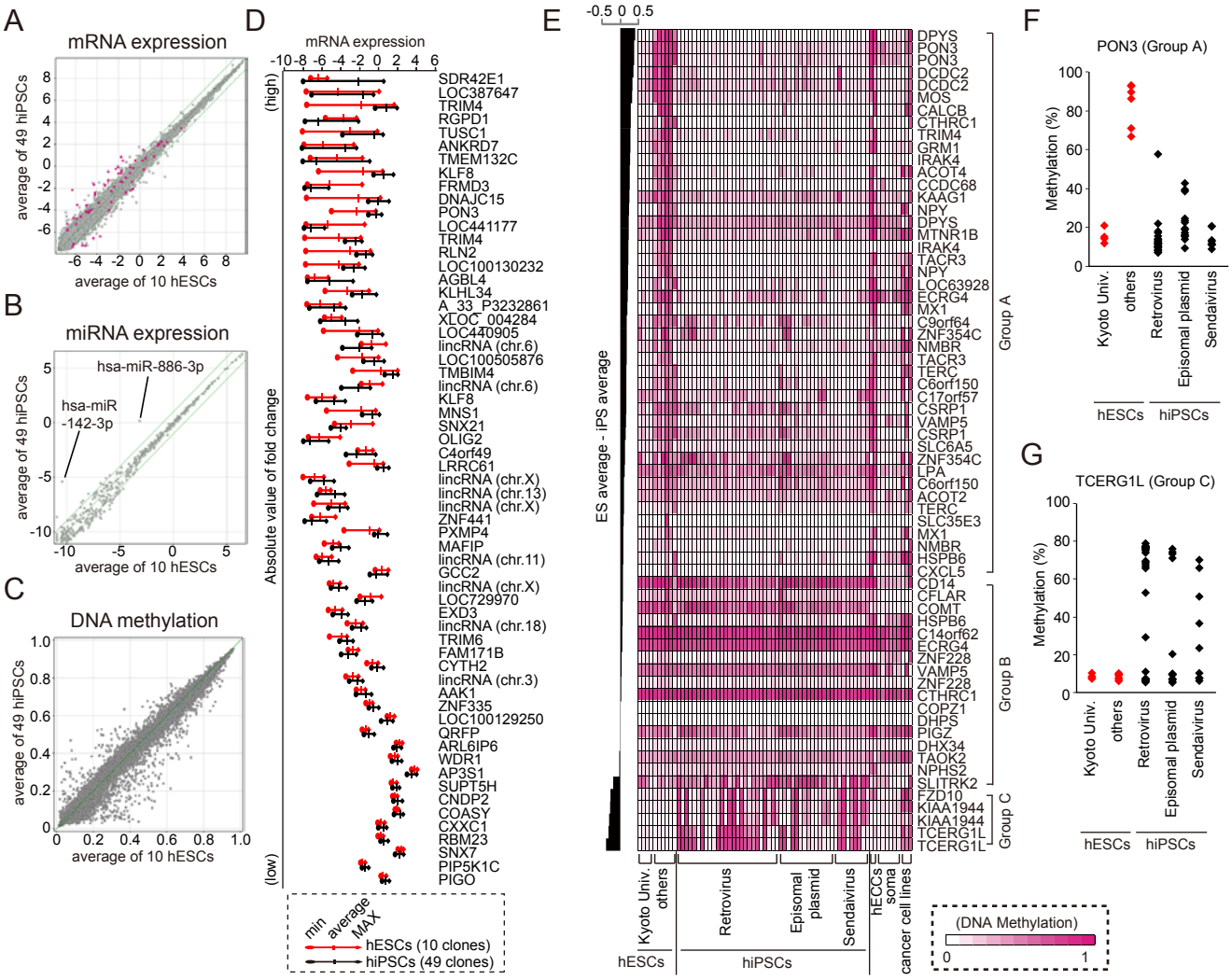

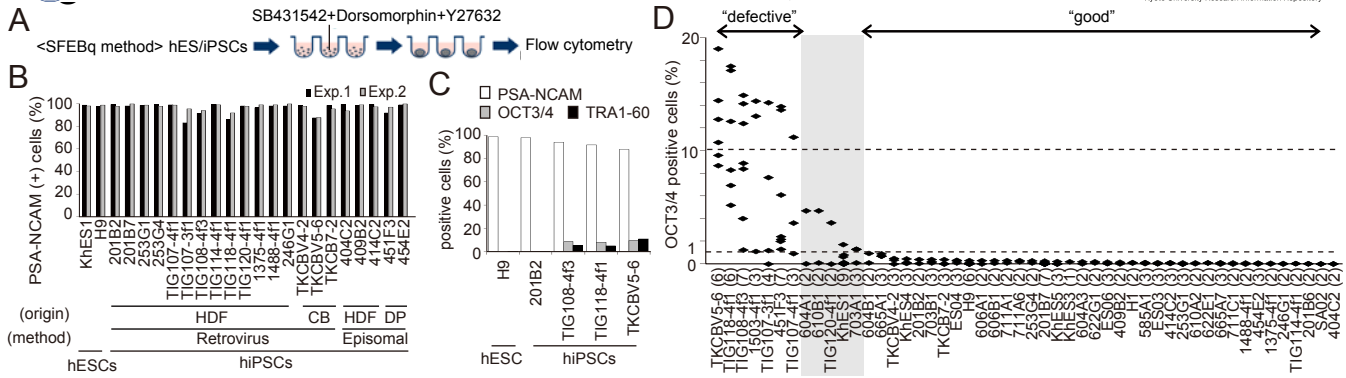

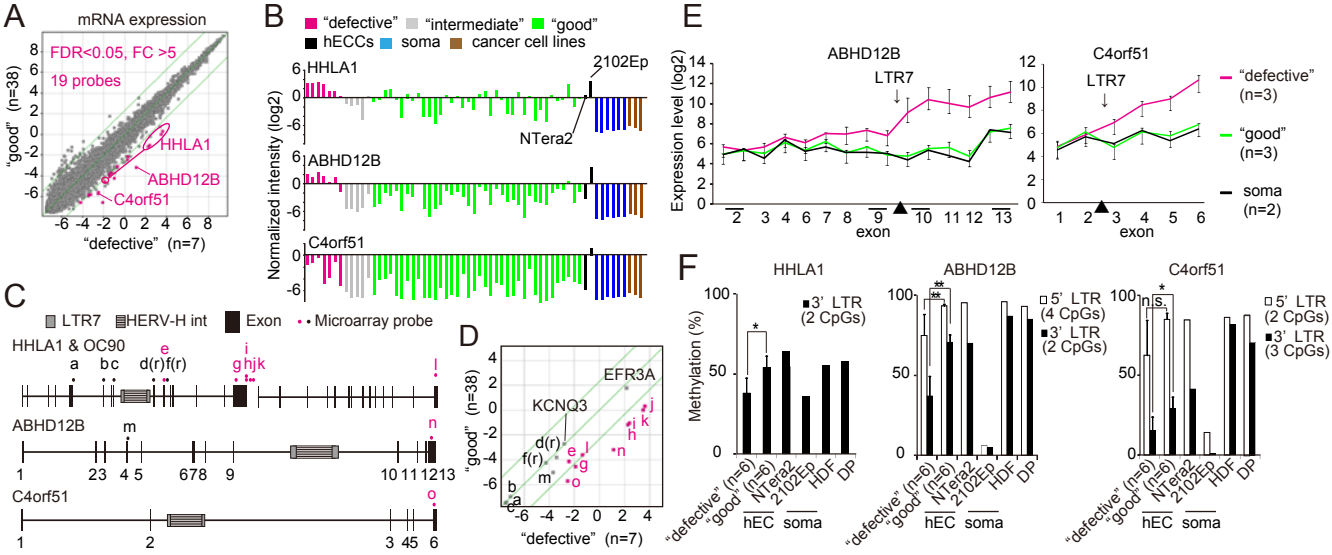

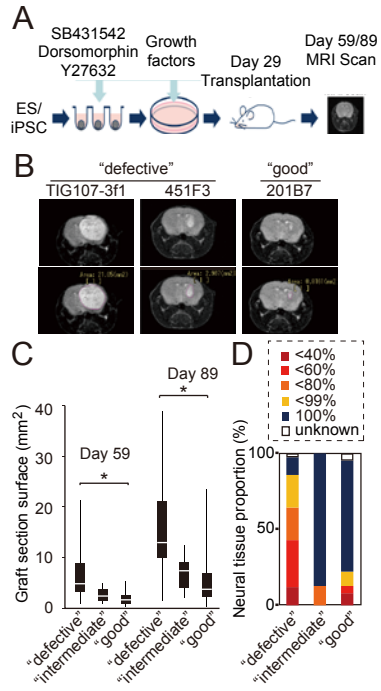

SI Material and Methods

Cell culture

The hESCs and hiPSCs were maintained in Primate ES cell medium (ReproCELL) supplemented with 4 ng/ml of human recombinant basic fibroblast growth factor (bFGF, Wako) on SNL feeders (1-3). Human dermal fibroblasts (HDFs) were obtained from the Japanese Collection of Research Bioresources (JCRB) or were purchased from Cell Applications, Inc. Dental pulp (DP) cells were kindly provided by Dr. Ken-ichi Tezuka (Gifu University Graduate School of Medicine). HDFs and hECC lines were maintained in Dulbecco's modified Eagle medium (DMEM, Nacalai tesque) containing 10% fetal bovine serum (FBS, Thermo) and 0.5% Penicillin/Streptomycin (Pen/Strep, Life Technologies). DP cells were cultured in MSBGM medium (Lonza). $CD34^+$ cord blood cells were obtained from the Stem Cell Resource Network in Japan (Banks at Miyagi, Tokyo, Kanagawa, Aichi, and Hyogo) through the RIKEN BioResource Center (Tsukuba, Ibaraki, Japan). The peripheral blood was harvested from healthy donors whose written informed consent was obtained in accordance with the institutional review board requirements. The mononuclear cells were then isolated by density gradient centrifugation with Ficoll-paque plus (GE healthcare).

Generation of human iPSCs

The generation of hiPSCs from HDFs, DP cells and blood samples using a retroviral system or episomal vectors was performed as described previously (1, 4-6). TKCBV4-2, 5-6 and TKCB7-2 iPS cells were kindly provided by Drs. Koji Eto and Naoya Takayama (7).

During the generation of hiPSCs from blood using Sendai viral vectors, vectors encoding OCT3/4, SOX2, KLF4 and c-MYC (CytoTune-iPS, DNAVEC) were infected into $CD34^+$ cells at a multiplicity of infection of 3 or 10 in αMEM medium supplemented with 10% FBS, 50 ng/ml IL-6, 50 ng/ml sIL-6R, 50 ng/ml SCF, 10 ng/ml TPO, 20 ng/ml Flt3 ligand and 20 ng/ml IL-3. The next day, the infected cells were centrifuged to remove residual virus, plated onto 6-well plates covered with MEF feeder cells and cultured in Primate ES cell medium supplemented with 4 ng/ml of bFGF until colonies were formed. Sendai virus infection and the generation of iPSCs from αβT cells were carried out as described previously (8).

RNA extraction

We lysed the cells at subconfluent density using the Trizol reagent (Life Technologies), and total RNA was purified by a standard protocol. The RNA

concentration and purity were determined through measurement of the A260/280 ratios with a Nanodrop instrument (Thermo Scientific). For microarrays, confirmation of the RNA quality was performed using the Agilent 2100 Bioanalyzer (Agilent Technologies).

mRNA expression analysis

The gene expression profiling was carried out using the SurePrint G3 Human GE Microarray (Agilent) according to the manufacturer's protocol. The data were analyzed using the Gene spring GX 11.5.1 software program (Agilent Technologies). The data processing was performed as follows: (i) Threshold raw signals were set to 1.0, (ii) Log base 2 transformation was performed, (iii) 75th percentile normalization was chosen as the normalized algorithm (http://genespring-support.com/faq/normalization). The flag setting was performed as follows: feature is not positive and significant (not detected), not uniform (compromised), not above background (not detected), saturated (compromised) or is a population outlier (compromised). Control probes were removed and only the "detected" probes that were present in at least one sample in all hES/hiPS cell samples were used for the further analysis. The number of probes used in the analysis was 36,757 (**Fig. 1A**) and 36,083 (**Fig. 3A**).

microRNA microarray analysis

The miRNA expression profiling was carried out using the Agilent Human miRNA microarray Rel 12.0 according to the manufacturer's protocol. The data were analyzed using the Gene spring GX 11.5.1 software program (Agilent Technologies) and data processing was performed in the same way as for the mRNA expression analysis, except that 90th percentile normalization was chosen as the normalized algorithm. The number of probes used in the analysis was 476 (**Fig. 1B**).

Genomic DNA extraction and bisulfite treatment

Genomic DNA extraction and purification from cultured cells was carried out using a Gentra Puregene kit (QIAGEN). Extracted DNA was quantitated by using the Nanodrop instrument, and the quality was assessed by gel electrophoresis. A total of 500 ng of genomic DNA was treated with bisulfite using the EZ DNA Methylation-Gold Kit (Zymo Research Corp., Irvine, CA) according to the manufacturer's protocol.

DNA methylation analysis with a beads-array

Genome-wide DNA methylation profiling was performed using the Illumina Infinium Human Methylation27 BeadChip (Illumina). Bisulfite-converted DNA was

used, and the remaining assay steps were performed using the reagents supplied by Illumina and their specified conditions. The readout from the array was a β-value, which was defined as the ratio between the fluorescent signal from the methylated allele to the sum of both methylated and unmethylated alleles, and thus correlated with the level of DNA methylation. A β-value of 1.0 corresponds to complete methylation and 0 is equal to no DNA methylation. To exclude potential sources of technical bias, we only used CpG sites with detection P values < 0.05 in at least 56 out of 59 samples. Normalization was not performed. The number of probes used in the analysis was 27,445 (**Fig. 1E**).

Generation of heat maps

We used Microsoft Excel to visualize the values as heat maps. The color spectrum expands from green (lower value) to magenta (higher value) through black in the gene/miRNA expression analysis, and from white (hypomethylation) to magenta (hypermethylation) in the DNA methylation analysis.

Bioinformatic analysis

A hierarchical clustering analysis was performed using the Gene Spring GX 11.5.1 software program.

DNA methylation analysis with pyro- and clonal- sequencing

Pyrosequencing was carried out with primers designed using the Pyromark Assay Design Software program, ver. 2.0 (QIAGEN). The primer sequences are shown in **Table S1D**. PCR was performed in a 25 μL reaction mixture containing 25 ng bisulfite-converted DNA, 1X Pyromark PCR Master Mix (QIAGEN), 1X Coral Load Concentrate and 0.2 μM forward and 5' biotinylated reverse primers. The PCR conditions were 45 cycles of 95°C for 30s, 56°C for 30s and 72°C for 30s. The PCR product was bound to streptavidin sepharose beads (GE Healthcare, Uppsala, Sweden), and was purified, washed, denatured and washed again. Then, 0.4 μM of the sequencing primer was annealed to the purified PCR product. Pyrosequencing reactions were performed using the PSQ HS 96 Pyrosequencing System. The degree of methylation is shown as the percentage of methylated cytosines divided by the sum of methylated and unmethylated cytosines (percentage of 5mC). Bisulfite-clonal sequencing was performed as previously described (9). In **Fig. 4F** and **Fig. S3C**, we examined the DNA methylation status of LTR7 and its neighboring regions in "defective" clones with high expression levels of these genes (n = 6; TKCBV5-6, TIG118-4f1, TIG108-4f3, 1503-4f1, TIG107-3f1 and 451F3), "good" clones with low expression levels of these genes (n =

6; 703B1, 606B1, 201B7, H1, 253G1 and 454E2), two hECC lines (NTera2 and 2102Ep) and two somatic cell lines (HDF and DP).

Exon arrays

We performed the exon array of the *ABHD12B* and *C4orf51* genes for three "defective" clones with high expression levels of these genes (n=3, TKCBV5-6, TIG108-4f3 and 451F3), three "good" clones with low expression levels of these genes (n=3, 201B7, H1 and 253G1) and somatic cells (HDF and DP74). cDNA was generated with the WT expression kit (Ambion) per the manufacturer's instructions. The cDNA was fragmented and end-labeled with a GeneChip WT Terminal labeling kit (Affymetrix). Approximately 5.5 μg of labeled DNA target was hybridized to the Affymetrix GeneChip Human Exon 1.0 ST Array at 45°C for 17 h, per the manufacturer's recommendations. Hybridized arrays were washed and stained on a GeneChip Fluidics Station 450 and scanned on a GCS3000 Scanner (Affymetrix). An exon array data analysis was performed using the Gene Spring GX11.5.1 software program employing ExonPLIER16 with core and extended probe sets. The exon probe sets were accepted if they had a DABG p-value < 0.05 in at least one of the samples.

Selection of microarray probes related to LTR7

The RepeatMasker database classifies sequences into subgroups by *in silico* analysis. We used LTR7 sequences registered in Repeatmasker open 3.3.0 – Repeat Library 20110920, a database of human repetitive sequence (http://www.repeatmasker.org/species/homSap.html). According to this database, there are 3523 LTR7 elements, including LTR7A, 7B, 7C in the human genome. In order to extract microarray probes that were potentially affected by LTR7 elements, we first selected genes containing LTR7 elements in their gene bodies or in the regions 2 kb upstream from their transcription start sites. We then extracted microarray probes that were located between the each LTR7 and the 3' end of the corresponding gene body (The direction of LTR7 was not considered). As a result, we extracted 763 probes corresponding to 435 genes from the Agilent human G3 microarray as LTR7-related probes (**Table S1C**).

Quantitative RT-PCR

To remove any potential contamination by genomic DNA, we treated purified RNA samples with a Turbo DNA free kit (Ambion). After DNase treatment, reverse

transcription was performed with the oligo dT_{20} primer using a ReverTra Ace-α-kit (Toyobo). qRT-PCR was performed with SYBR Premix Ex Taq II (Takara), and samples were analyzed with the StepOne plus real-time PCR system (Applied Biosystems). The primer sequences are shown in **Table S1D**. The relative expression level was calculated by using plasmid DNA containing the PCR product (**Fig 4 and Figs S5C,D)**.

Neural induction

We performed the neural differentiation of human pluripotent stem cells with the quick method for serum-free embryoid body formation (SFEBq) as described previously (10). In brief, hESCs and hiPSCs treated with 10 μM Y-27632 were dissociated into single cells and transferred at 9000 cells per well to 96-well low cell adhesion plates (Lipidure-Coat Plate A-U96; NOF Corporation). The cells were cultured for 14 days in DFK5 medium consisting of DMEM/F-12 (Life Technologies), 5% Knockout Serum Replacement (KSR, Life Technologies), 1% MEM-non-essential amino acids (Life Technologies), 2 mM L-glutamine (Life Technologies), 0.1 mM 2-mercaptoethanol (Life Technologies) and 0.5% penicillin/streptomycin. We used DFK5 medium supplemented with 10 μM Y-27632, 2 μM dorsomorphin (SIGMA) and 10 μM SB431542 (SIGMA) for the first four days.

Adhering neural differentiation of Dual SMAD inhibition was performed as described previously (11). Briefly, the cells were plated on matrigel-coated plate and after reaching to 90% confluency, they were cultured with 100 nM LDN193189 (Stemgent), 10 μM SB431542 in 15% knockout serum replacement, 2 mM L-glutamine and 10 μM β-mercaptoethanol-conteining D-MEM for 12 days.

For dopaminergic differentiation, we first transferred ESCs or iPSCs onto 96-well low cell adhesion plates with Y-27632, dorsomorphin and SB431542 in the same way as indicated for SFEBq. We supplemented the cultures with 100 ng/ml FGF8 (Peprotech) and 20 ng/ml WNT1 (Peprotech) from day five to 12, and with 200 ng/ml SHH (R&D) from day eight to 12. Twelve days after induction, aggregates were transferred onto 6-well plates coated with laminin (Becton-Dickinson) and Poly-L-ornithine (SIGMA) and were cultured with Neurobasal medium (Life Technologies) containing 2% B27 supplement (Life Technologies), 2 mM L-glutamine and 0.5% penicillin/streptomycin. We added 200 ng/ml SHH to the medium from day 12 to 15, and 1 ng/ml FGF20 and 12.5 ng/ml bFGF from day 15 to 22. On day 22, the cells were dissected into clumps and plated on new 6-well plates coated with laminin and Poly-L-ornithine, and were then cultured with Neurobasal medium supplemented with 2 ng/ml GDNF (R&D), 20 ng/ml BDNF (R&D), 400 mM dbcAMP (SIGMA) and 200 mM Ascorbic Acid

(SIGMA) until day 29. TRA-1-60-positive cell labeling and depletion were performed on day 22 using an Anti-TRA-1-60 MicroBead kit and the autoMACS pro device (Miltenyi Biotech).

Flow cytometric analysis

Neural aggregates were dissociated and processed for the flow cytometric analysis by a FACS Aria II instrument (Becton-Dickinson). To analyze the proportion of OCT3/4$^+$ cells, the cells were fixed with 3.7% formaldehyde, permeabilized with 0.2% TritonX-100 and stained with the appropriate antibody. To count the number of PSA-NCAM$^+$ cells or TRA-1-60$^+$ cells, cells were prepared without fixation. To eliminate the number of dead cells from the total cell population, we stained the cells with propidium iodide after labeling them with the anti-TRA-1-60 or anti-PSA-NCAM antibody, or with red fluorescent reactive dye from the LIVE/DEAD Fixable Dead Cell Stain Kits (Invitrogen) before fixing the cell suspension.

Transplantation of ES/iPS cell-derived dopaminergic neuron cultures into the brains of NOD/SCID mice

To prepare samples for injection, we scraped and mechanically dissected cells by

gently pipetting them up and down a few times, suspended them in culture medium (1 x 10^6 cells/μl) and injected 2 μl of the cell suspension into the right striatum (2 mm lateral, 1 mm rostral to the bregma; depth, 3 mm from the dura) of NOD/SCID mice (6 weeks old, female) using a glass micropipette, as described previously (12).

Magnetic resonance imaging

Graft imaging was performed with a MRmini SA instrument (DS Pharma Biomedical) by using a cylindrical slotted holder with a 20 mm radio frequency coil constructed for mice. T2-weighted images (repetition time = 2000 ms, echo time = 69 ms) were recorded. The brains were imaged coronally in a single section through the graft center by using an image matrix of 256 x 128, a field of view of 2 x 4 cm^2, and two excitations. Parametric images were generated by using the Sampler XP-NI software program (DS Pharma Biomedical). Graft section surfaces were measured by using the INTAGE Realia Professional imaging software program (CYBERNET).

Immunostaining

Anti-NCAM (ERIC1) antibody (Santa Cruz) was used as a primary antibody and anti-Mouse Ig Biotin (Dako) was used as a secondary antibody for

immunocytechemistry.

Statistical analysis

Gene/miRNA expression

We conducted the *t*-test (variances assumed equal) for the normalized, filtered data and controlled the false discovery rate (FDR) at 0.05 using the Benjamini-Hochberg method to identify probes that differed significantly between hESCs and hiPSCs, or for neural differentiation “good” and “defective” clones.

DNA methylation determined using the beads-array

We conducted Mann-Whitney’s U-test on the filtered data controlling the FDR at 0.05 using the Benjamini-Hochberg method to identify probes that differed significantly between hESCs and hiPSCs.

DNA methylation as determined by pyro- and clonal- sequencing

Mann-Whitney’s U-test was used to compare the quantitative methylation values between hESCs and hiPSCs or“defective” and “good” groups. Calculations were carried

out with the Statview software program.

Graft size after transplantation

The *t*-test was used to compare the graft sizes derived from "defective" and "good" clones (**Fig. 4C**). In the case of comparisons between graft sizes between unsorted and depleted cell cultures, we performed the paired *t*-test.

1. Takahashi K, *et al.* (2007) Induction of pluripotent stem cells from adult human fibroblasts by defined factors. *Cell* 131(5):861-872.
2. Fujioka T, Yasuchika K, Nakamura Y, Nakatsuji N, & Suemori H (2004) A simple and efficient cryopreservation method for primate embryonic stem cells. *Int J Dev Biol* 48(10):1149-1154.
3. Ohnuki M, Takahashi K, & Yamanaka S (2009) Generation and characterization of human induced pluripotent stem cells. *Curr Protoc Stem Cell Biol* Chapter 4:Unit 4A 2.
4. Okita K, *et al.* (2011) A more efficient method to generate integration-free human iPS cells. *Nat Methods* 8(5):409-412.
5. Tamaoki N, *et al.* (2010) Dental Pulp Cells for Induced Pluripotent Stem Cell Banking. *J Dent Res* 89(8):773-778.
6. Okita K, *et al.* (2013) An efficient nonviral method to generate integration-free human-induced pluripotent stem cells from cord blood and peripheral blood cells. *Stem Cells* 31(3):458-466.
7. Kajiwara M, *et al.* (2012) Donor-dependent variations in hepatic differentiation from human-induced pluripotent stem cells. *Proc Natl Acad Sci U S A* 109(31):12538-12543.
8. Seki T, *et al.* (2010) Generation of induced pluripotent stem cells from human terminally differentiated circulating T cells. *Cell Stem Cell* 7(1):11-14.
9. Takahashi K & Yamanaka S (2006) Induction of pluripotent stem cells from mouse embryonic and adult fibroblast cultures by defined factors. *Cell* 126(4):663-676.
10. Morizane A, Doi D, Kikuchi T, Nishimura K, & Takahashi J (2011) Small-molecule inhibitors of bone morphogenic protein and activin/nodal signals promote highly

efficient neural induction from human pluripotent stem cells. *J Neurosci Res* 89(2):117-126.

11. Kriks S, *et al.* (2011) Dopamine neurons derived from human ES cells efficiently engraft in animal models of Parkinson's disease. *Nature* 480(7378):547-551.
12. Miura K, *et al.* (2009) Variation in the safety of induced pluripotent stem cell lines. *Nat Biotechnol* 27(8):743-745.

Supplemental figure legends.

Fig. S1. Gene expression patterns among Kyoto hESCs, other hESCs and hiPSCs and DNA methylation levels of previously reported ES-iPS DMRs in our cell lines

(**A**) Heat maps showing the expression levels of 15 probes that were differentially expressed between hESCs and hiPSCs (FDR < 0.05 and absolute FC > 3) and hsa-miR-142-3p and hsa-miR-886-3p in various cell lines. A hierarchical clustering analysis for 15 probes was performed using the Euclidean distance and average linkage algorithm. (B) A hierarchical clustering analysis of the global gene expression patterns in various cell lines was performed using the Euclidean distance and average linkage algorithm in the Gene Spring GX 11.5.1 software program.

(C) Some previously reported hES-iPS DMRs; A2BP1, IGF1R, ZNF184, POU3F4 and PTPRT were examined by pyrosequencing in 10 hESCS, 49 hiPSCs in our laboratory. Each CpG dinucleotide position was assayed in triplicate, and average values were plotted. Mann-Whitney's U-test was used to compare the quantitative methylation

values between hESCs and hiPSCs. (n.s.; not significant, *; $p<0.05$, ** ; $p<0.01$)

Fig S2. Most of the cells can differentiate into neural cells although some clones retain undifferentiated cells after neural differentiation

(A) The expression levels of PAX6 (left panel) and MAP2 (right panel) in neurospheres of differentiated hESC line H9 and hiPSC lines (253G1, TIG108-4f3 and TKCBV5-6) were determined by quantitative RT-PCR. The expression levels in hESC line H9 before differentiation were set to 1, and relative expression levels were presented in log scale.

(B) A comparison of the proportion of TRA-1-60-positive cells after neural induction between the SFEBq method (white) and the adhesion culture method (black).

Fig. S3. Activation of LTR7 is not confined to HHLA1, ABHD12B and C4orf51; DNA hypomethylation exists in some, but not all, of LTR7s in “defective” hiPSC clones.

(A) The extraction of 763 probes corresponding to 435 genes as LTR7-related probes from the Agilent human G3 microarray (design ID 028004). (B) A comparison of the expression levels of 763 LTR7-related probes between “good” and “defective” clones. Magenta-colored genes (ABHD12B, HHLA1 and C4orf51) and yellow-colored genes (ARRB1, FAAH2 and TBC1D23) are differentially expressed between the “good” and “defective” clones (FDR < 0.05 and FC >5 or FC>2,

respectively) and green-colored genes (DNMT3B, ABCA1 and APP) did not show any differences. (C) The DNA methylation status of LTR7 and its neighboring regions of ARRB1, FAAH2 and TBC1D23 were examined by pyro-sequencing and those of DNMT3B, ABCA1 and APP were examined by clonal-sequencing. Mann-Whitney's U-test was used to compare the quantitative methylation values between "defective" and "good" clones (n.s.; not significant, *; $p<0.05$).

Fig. S4. The histology of grafts derived from hESCs and hiPSCs

(A) Transplanted mouse brains were fixed with formaldehyde, embedded in paraffin, sectioned, and stained with hematoxylin and eosin (HE). The ratios indicate neural cells and non-neural cells as determined by a microscopic observation. Scale bar, 500 μm.

(B) HE-stained sections (left panel) and human NCAM-stained sections (right two panels) of mouse brains transplanted with 29 day-differentiated hESC/iPSCs. (C) The maximum surface size of graft sections 45 or 60 days after transplantation. Transplanted cells were prepared with or without depletion of TRA-1-60^{+} cells 22 days after differentiation. *t-test, paired $p<0.05$

Fig. S5 High expression levels of the hsa-mir-371-373 cluster, KLF4 and transgenes are not absolute markers for "type 1 defectiveness"

The expression levels of hsa-mir-371-373 (A) and KLF4 (B) were examined by a microarray analysis in seven “defective” clones, five “intermediate” clones, 38 “good” clones, two hECC lines (NTera2 and 2102Ep), six somatic cell lines (HDF, DP, CB1,CB2, PBMN1, PBMN2) and three cancer cell lines (HepG2, MCF7 and Jurkat). The total and retroviral transgene expression levels of KLF4 (C) and OCT3/4 (D) were measured by qPCR in 18 hiPS clones established by a retroviral method, the “defective” clone 451F3, which was generated using an episomal plasmid vector, four hESCs, two hECCs and two somatic cell lines (HDF, DP).

Fig. S6. previously reported iPS-specific aberrantly methylated genes’ expressions

A heat map for 10 hESCs and 49 hiPSCs examined in our laboratory based on the gene expression levels of reported aberrantly methylated genes that can distinguish hiPSCs and hESCs. Of nine previously reported genes, probes for C22ORF34 were “not detected” in all the samples in our microarray platform, so we only evaluated the other 8 genes (8 probes, “detected” in at least two clones of our samples).

Figure S1

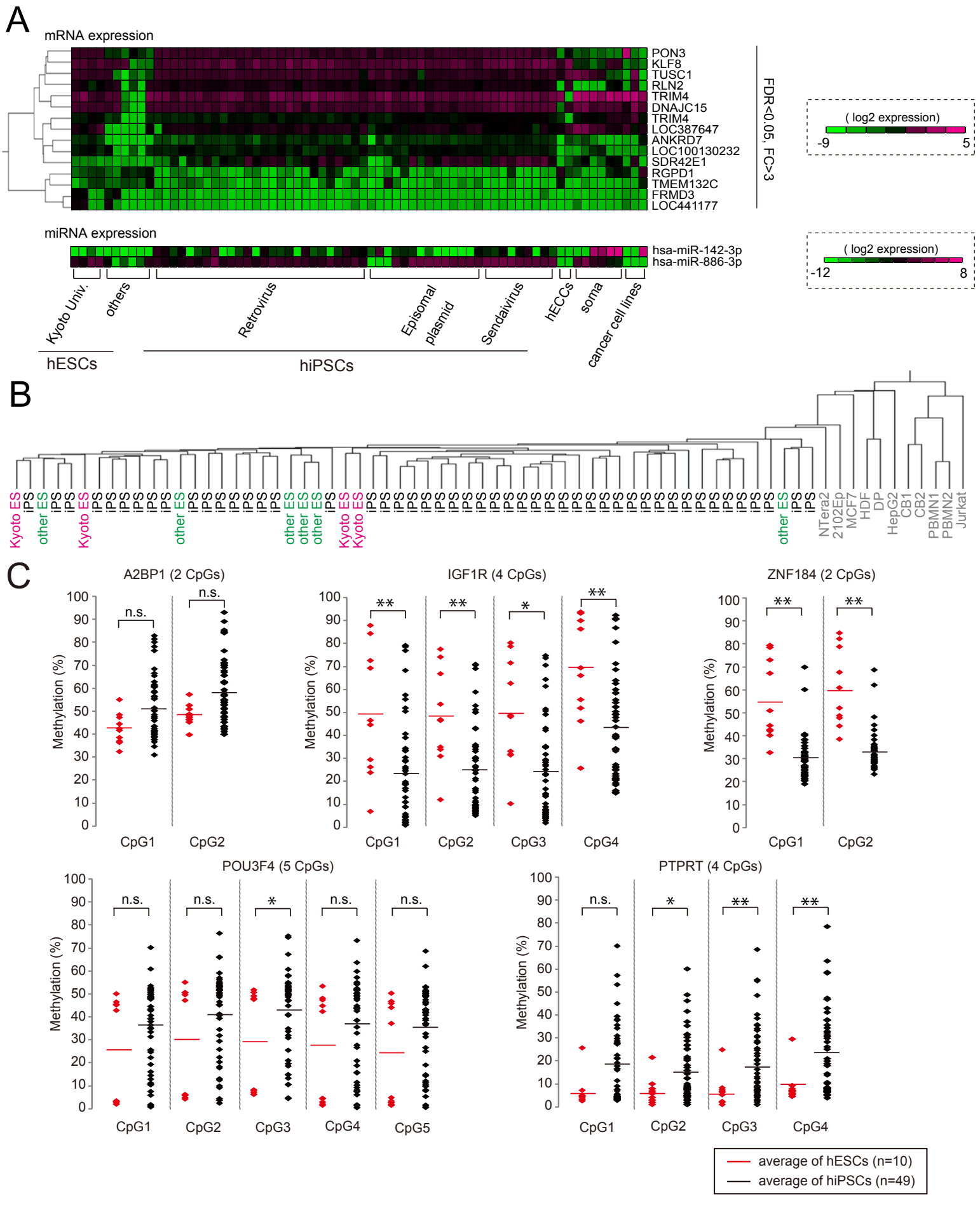

Figure.32

A

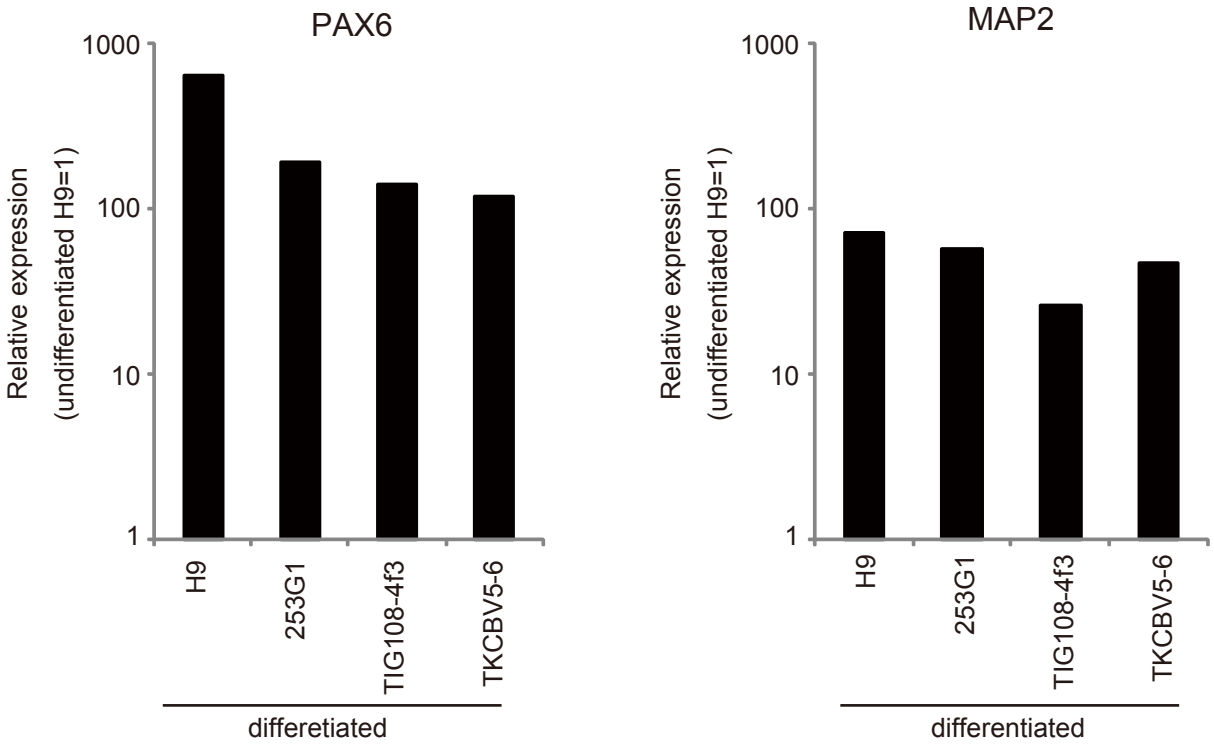

B

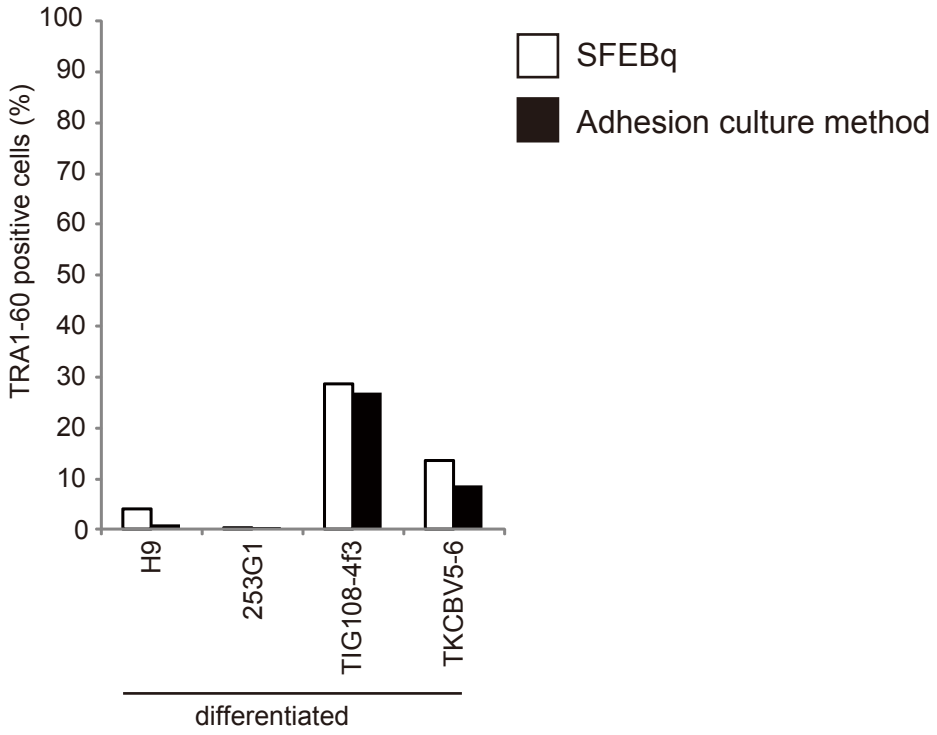

Figure.S3

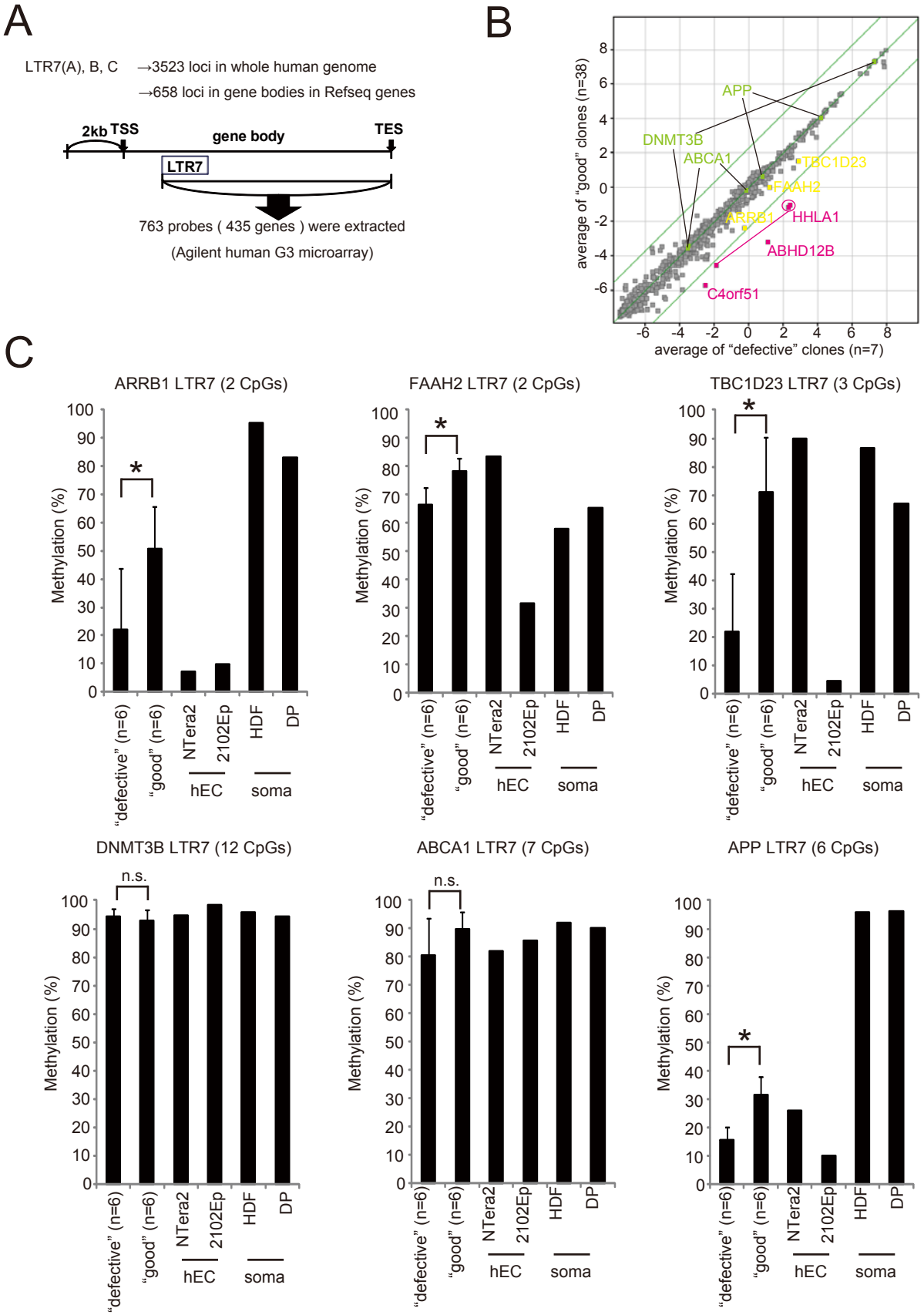

Figure S4

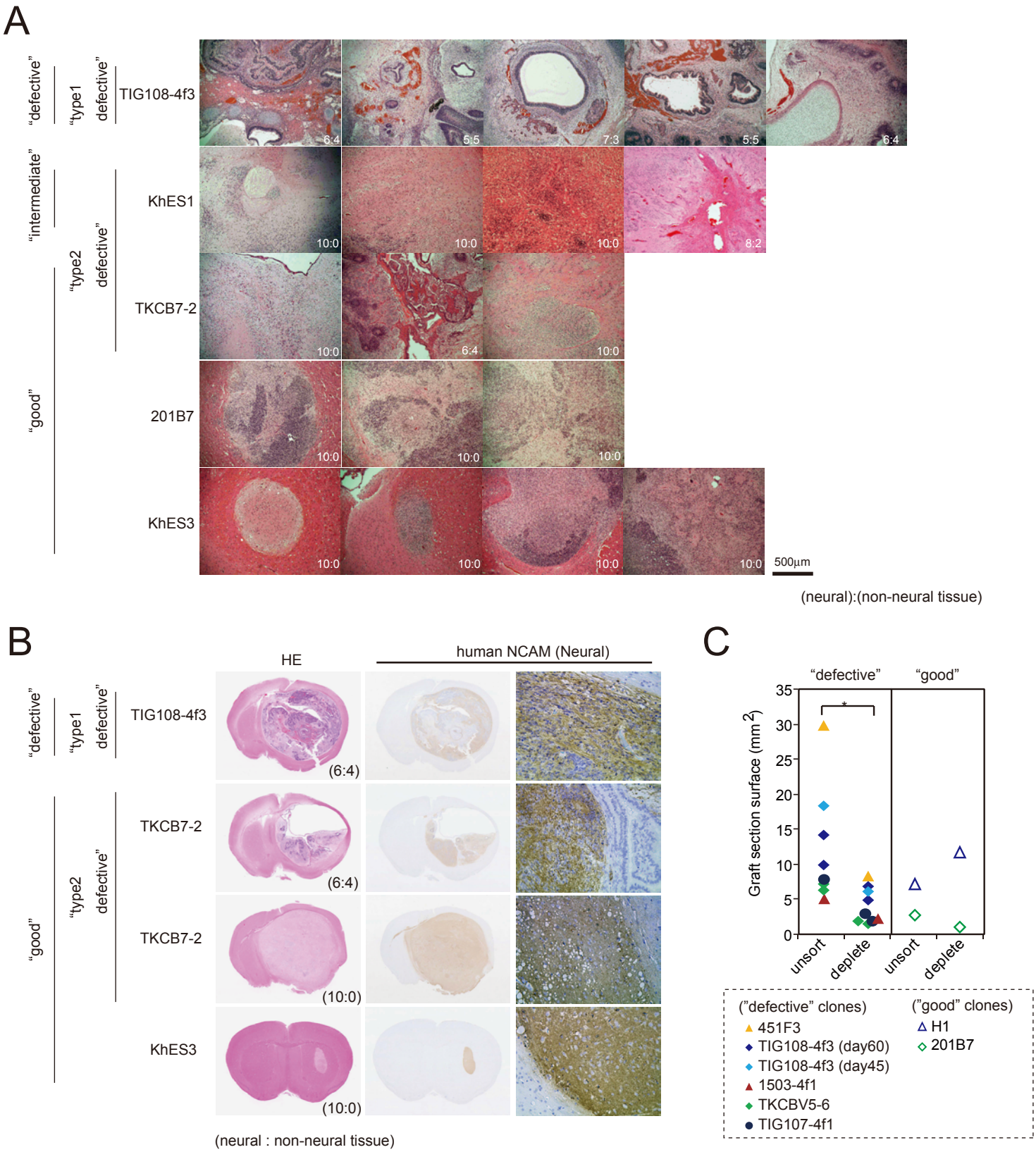

Figure 35

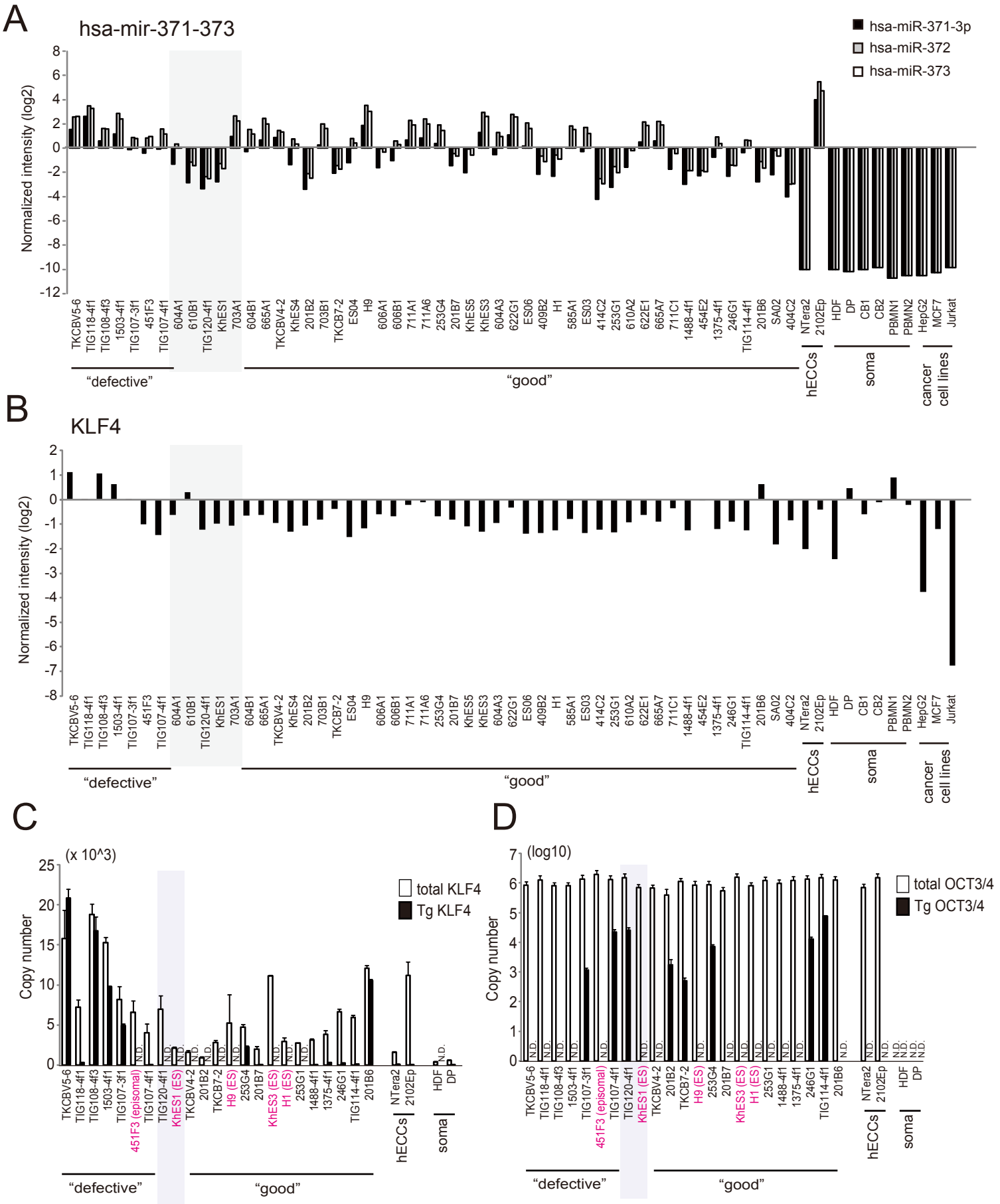

Figure. S6

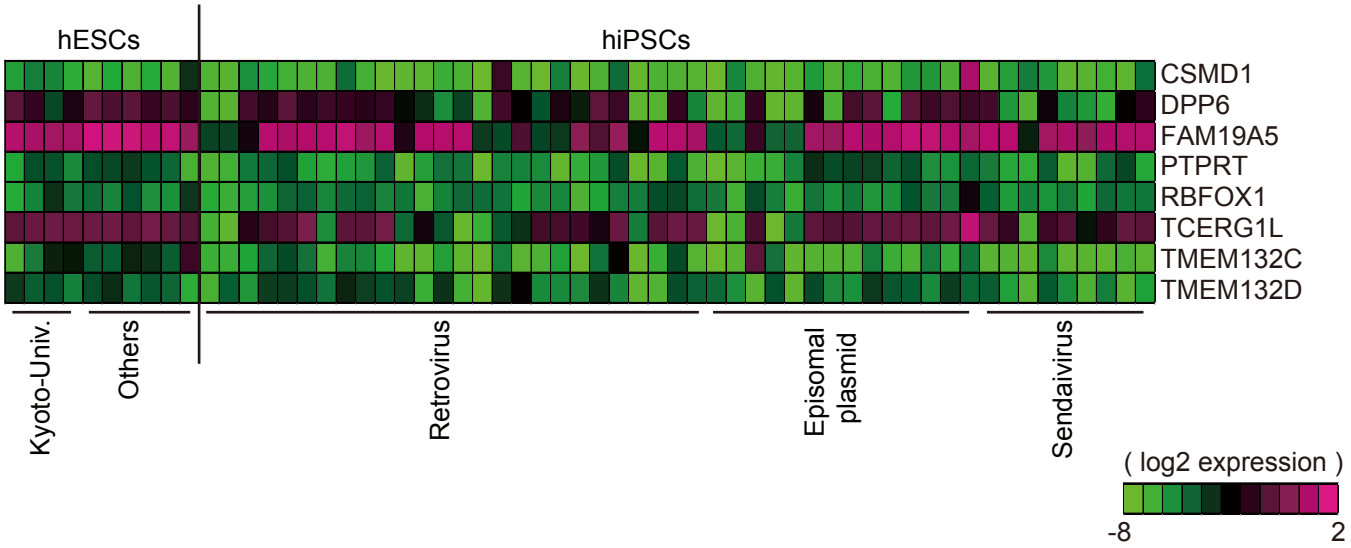

Table S1A. List of CpGs reported as differentially methylated between hESCs and hiPSCs (only covered by the infinium platform)

		Chromosomal Coordinates (hg19 version)					
cg number (infinium)	gene symbol	Chr. number	position of CpG (infinium)	start	end	reference	reported methylation status
cg23045073	NPHS2	chr1	179545458	179545343	179546543	Doi et al., 2009	ES < iPS
cg13722123	GRM1	chr6	146350346	146349702	146350414		ES > iPS
cg22411207	MOS	chr8	57026301	57025648	57026328		ES > iPS
cg27205791	COPZ1	chr12	54719080	54718379	54719446		ES > iPS
cg10316764	TAOK2	chr16	29984665	29984318	29984860		ES < iPS
cg21756353	DHPS	chr19	12792451	12791946	12792452		ES > iPS
cg03257423	ZNF228	chr19	44860820	44860544	44862008		ES > iPS
cg23850272	ZNF228	chr19	44861241	44860544	44862008		ES > iPS
cg03000603	DHX34	chr19	47852595	47852502	47853505		ES > iPS
cg03020597	SLITRK2	chrX	144898810	144897718	144898947		ES < iPS
cg11108890	VAMP5	chr2	85811471	85811204	85812203	Lister et al., 2010	ES > iPS
cg25651505	VAMP5	chr2	85812023	85811204	85812203		ES > iPS
cg11024597	ECRG4	chr2	106681411	106681383	106682982		ES > iPS
cg10885338	ECRG4	chr2	106682640	106681383	106682982		ES > iPS
cg17802847	CFLAR	chr2	201980910	201980570	201982169		ES > iPS
cg27020690	TERC	chr3	169482358	169482261	169483360		ES > iPS
cg01389761	TERC	chr3	169482968	169482261	169483360		ES > iPS
cg00936626	PIGZ	chr3	196694856	196693558	196695157		ES > iPS
cg10088985	CXCL5	chr4	74864313	74863700	74864699		ES > iPS
cg04263186	TACR3	chr4	104640489	104640415	104642014		ES > iPS
cg05389335	TACR3	chr4	104641319	104640415	104642014		ES > iPS
cg25358289	CD14	chr5	140012728	140011238	140012837		ES > iPS
cg11538128	ZNF354C	chr5	178487481	178487016	178488015		ES > iPS
cg04488521	ZNF354C	chr5	178487716	178487016	178488015		ES > iPS
cg08126211	KAAG1	chr6	24357720	24357674	24358773		ES > iPS
cg04515001	DCDC2	chr6	24358236	24357674	24358773		ES > iPS
cg16306115	DCDC2	chr6	24358306	24357674	24358773		ES > iPS
cg00463577	C6orf150	chr6	74161911	74160732	74162431		ES > iPS
cg09527362	C6orf150	chr6	74162142	74160732	74162431		ES > iPS
cg08109815	NMBR	chr6	142409831	142409560	142410659		ES > iPS
cg17256157	NMBR	chr6	142410100	142409560	142410659		ES > iPS
cg07260592	LPA	chr6	161100122	161099863	161100862		ES > iPS
cg05158615	NPY	chr7	24323559	24323459	24325058		ES > iPS
cg12614105	NPY	chr7	24324435	24323459	24325058		ES > iPS
cg10329418	PON3	chr7	95026181	95025448	95026447		ES > iPS
cg24750391	PON3	chr7	95026211	95025448	95026447		ES > iPS
cg26952662	CTHRC1	chr8	104383499	104383030	104384629		ES > iPS
cg19188612	CTHRC1	chr8	104384291	104383030	104384629		ES > iPS

cg10303487	DPYS	chr8	105479058	105478430	105479429		ES > iPS
cg20774846	DPYS	chr8	105479420	105478430	105479429		ES > iPS
cg10175795	TCERG1L	chr10	133109194	133108510	133111409		ES < iPS
cg03943081	TCERG1L	chr10	133110646	133108510	133111409		ES < iPS
cg08896945	CALCB	chr11	15095068	15094797	15096396		ES > iPS
cg11784785	SLC6A5	chr11	20620089	20618097	20620296		ES > iPS
cg15842276	MTNR1B	chr11	92702648	92702225	92703224		ES > iPS
cg20424530	IRAK4	chr12	44152509	44151863	44153462		ES > iPS
cg08992050	IRAK4	chr12	44152940	44151863	44153462		ES > iPS
cg20360244	SLC35E3	chr12	69140065	69139863	69140962		ES > iPS
cg03469054	KIAA1944	chr12	130387861	130386777	130389576		ES < iPS
cg13234863	KIAA1944	chr12	130389138	130386777	130389576		ES < iPS
cg23054883	FZD10	chr12	130647580	130643277	130649076		ES < iPS
cg14912575	C14orf162	chr14	70038236	70038201	70039200		ES > iPS
cg00815605	ACOT2	chr14	74035882	74035701	74037300		ES > iPS
cg26780333	ACOT4	chr14	74058972	74058301	74059300		ES > iPS
cg15309006	LOC63928	chr16	23766116	23765733	23766732		ES > iPS
cg08085267	C17orf57	chr17	45401833	45401491	45402590		ES > iPS
cg07177852	CCDC68	chr18	52626476	52625891	52626890		ES > iPS
cg24673765	HSPB6	chr19	36247869	36246382	36248581		ES > iPS
cg15125472	HSPB6	chr19	36248077	36246382	36248581		ES > iPS
cg15925792	MX1	chr21	42798131	42797679	42799278		ES > iPS
cg22152328	MX1	chr21	42798386	42797679	42799278		ES > iPS
cg00540544	CSRP1	chr1	201476297	201475983	201476336	Ohi et al., 2011	ES > iPS
cg17780098	CSRP1	chr1	201476311	201475983	201476336		ES > iPS
cg01626227	TRIM4	chr7	99517289	99516971	99517450		ES > iPS
cg12927772	C9orf64	chr9	86571585	86571560	86571999		ES > iPS
cg23268677	COMT (TXNRD2)	chr22	19929097	19929072	19929357		ES > iPS

Table S1B. List of probes which showed differentially expression between 38 "good" clones and 7 "defective" clones (FC>5, FDR<0.05)

Putative transcript cluster	ProbeName	GeneSymbol	Description	Genomic Coordinates	Chromosome Strand_Avadis_
1	A_23_P417821	DMRTB1	Homo sapiens DMRT-like family B with proline-rich C-terminal, 1 (DMRTB1), mRNA [NM_033067]	chr1:53933088-53933147	+
2	A_33_P3236436	C4orf51	Homo sapiens chromosome 4 open reading frame 51 (C4orf51), mRNA [NM_001080531]	chr4:146653856-146653915	+
3	A_19_P00316694	XLOC_005614	BROAD lincRNAs version v2 (http://www.broadinstitute.org/genome_bio/human_lincrnas/)	chr6:14281107-14281048	-
	A_19_P00320902		lincRNA:chr6:14283301-14285685 reverse strand	chr6:14284343-14284284	-

	A_19_P00321571		lincRNA:chr6:14283035-14285450 reverse strand	chr6:14285417-14285358	-
4	A_33_P3297020	PSORS1C3	Homo sapiens psoriasis susceptibility 1 candidate 3 (non-protein coding) (PSORS1C3), non-coding RNA [NR_026816]	chr6:31141572-31141513	-
5	A_32_P3955	C7orf57	Homo sapiens chromosome 7 open reading frame 57 (C7orf57), mRNA [NM_001100159]	chr7:48099967-48100026	+
6	A_19_P00329841		lincRNA:chr7:124873114-124899839 reverse strand	chr7:124873767-124873708	-
7	A_19_P00331472		lincRNA:chr8:129599518-129624118 reverse strand	chr8:129599638-129599579	-
8	A_33_P3301050	HHLA1	Homo sapiens HERV-H LTR-associating 1 (HHLA1), mRNA [NM_001145095]	chr8:133073792-133073733	-
	A_19_P00325595		lincRNA:chr8:133071643-133092468 reverse strand	chr8:133073545-133073486	-
	A_19_P00330523		lincRNA:chr8:133071643-133092468 reverse strand	chr8:133073455-133073396	-
	A_19_P00321436	(HHLA1)	lincRNA:chr8:133073732-133075753 reverse strand	chr8:133073792-133073733	-
	A_19_P00319204	(HHLA1)	lincRNA:chr8:133076031-133093351 reverse strand	chr8:133076236-133076177	-
9	A_19_P00327099		lincRNA:chr8:138387843-138421643 reverse strand	chr8:138395981-138395922	-
10	A_23_P366035	ABHD12B	Homo sapiens abhydrolase domain containing 12B (ABHD12B), transcript variant 1, mRNA [NM_001206673]	chr14:51371212-51371271	+
11	A_19_P00325604		lincRNA:chr18:54721302-54731677 reverse strand	chr18:54722409-54722350	-
12	A_23_P38959	VAV1	Homo sapiens vav 1 guanine nucleotide exchange factor (VAV1), mRNA [NM_005428]	chr19:6853995-6854054	+
13	A_23_P432352	CXorf61	Homo sapiens chromosome X open reading frame 61 (CXorf61), mRNA [NM_001017978]	chrX:115593025-115592966	-

Table S1C. List of LTR7-related probes from the Agilent human G3 microarray (design ID 28004)

Probename	Genesymbl_in_Array	Genesymbl_in_refseq	chromosome	Probe_start	Probe_end
A_33_P3313258	ATAD3B	ATAD3B	chr1	1417934	1417993
A_33_P3396553	LOC732419	ATAD3B	chr1	1423229	1423288
A_33_P3331588	ATAD3B	ATAD3B	chr1	1431507	1431566
A_33_P3385477	ATAD3B	ATAD3B	chr1	1431522	1431581
A_23_P103942	DNAJC11	DNAJC11	chr1	6694205	6694234
A_33_P3271387	THAP3	DNAJC11	chr1	6695557	6695616
A_33_P3241108	DNAJC11	DNAJC11	chr1	6712909	6712968
A_23_P126623	PGD	PGD	chr1	10478911	10478970
A_33_P3307960	AADACL3	AADACL3	chr1	12785904	12785963
A_33_P3307965	AADACL3	AADACL3	chr1	12788667	12788726
A_23_P34597	CDA	CDA	chr1	20945069	20945128
A_24_P353619	ALPL	ALPL	chr1	21903084	21903884
A_23_P104146	ZMYM4	ZMYM4	chr1	35887010	35887069
A_23_P85640	INPP5B	INPP5B	chr1	38327872	38327931
A_33_P3216694	HIVEP3	HIVEP3	chr1	41975685	41975744
A_23_P383118	ZSWIM5	ZSWIM5	chr1	45482274	45482333
A_23_P51660	MUTYH	MUTYH	chr1	45794999	45795058
A_23_P126057	SCP2	SCP2	chr1	53516467	53516526
A_24_P491397	LDLRAD1	LDLRAD1	chr1	54474512	54474571
A_33_P3332406	LDLRAD1	LDLRAD1	chr1	54474691	54474750
A_23_P23850	DAB1	DAB1	chr1	57480639	57480698
A_33_P3375334	NOGENE	DAB1	chr1	57536473	57536532
A_32_P108655	AK3L1	AK4	chr1	65692632	65692691
A_32_P95067	AK3L1	AK4	chr1	65694099	65694158
A_23_P33093	ST6GALNAC5	ST6GALNAC5	chr1	77516413	77516472
A_33_P3315258	CHD1L	CHD1L	chr1	146736128	146736187
A_23_P45831	CHD1L	CHD1L	chr1	146766111	146766170
A_24_P336759	MCL1	MCL1	chr1	150547622	150547681
A_33_P3272952	LOC100131311	MCL1	chr1	150552070	150552129
A_23_P74309	NOS1AP	NOS1AP	chr1	162337975	162338034
A_19_P00813176	NOGENE	LOC100506023	chr1	173208439	173208498
A_19_P00807358	NOGENE	LOC100506023	chr1	173222254	173222313
A_19_P00813450	NOGENE	LOC100506023	chr1	173222232	173222291
A_33_P3391120	LOC646870	LOC100506023	chr1	173331503	173331562
A_19_P00328574	NOGENE	LOC100506023	chr1	173382628	173382687
A_19_P00811661	NOGENE	LOC100506023	chr1	173387004	173387063
A_19_P00805950	NOGENE	LOC100506023	chr1	173386997	173387056
A_19_P00317897	NOGENE	LOC100506023	chr1	173387179	173387238
A_32_P52119	NOGENE	LOC100506023	chr1	173387368	173387427
A_19_P00316156	NOGENE	LOC100506023	chr1	173387476	173387535
A_19_P00328176	NOGENE	LOC100506023	chr1	173387703	173387762
A_33_P3350758	RASAL2	RASAL2	chr1	178442587	178442646
A_23_P502747	RASAL2	RASAL2	chr1	178443038	178443097

A_32_P176594	KIAA1614	KIAA1614	chr1	180913533	180913592
A_23_P148990	HMCN1	HMCN1	chr1	186159679	186159738
A_23_P11685	PLA2G4A	PLA2G4A	chr1	186957652	186957711
A_33_P3311373	LOC401980	LOC401980	chr1	202955580	202955639
A_23_P149664	TMEM183B	TMEM183B|TMEM183A	chr1	202992196	202992255
A_23_P256821	CR1	CR1	chr1	207813016	207813075
A_33_P3338634	SYT14	SYT14	chr1	210334193	210334252
A_24_P402415	SYT14	SYT14	chr1	210335095	210335154
A_33_P3221683	C1orf227	C1orf227	chr1	213003515	213003574
A_33_P3321919	C1orf227	C1orf227	chr1	213009418	213009477
A_33_P3212949	USH2A	USH2A	chr1	215796333	215796392
A_19_P00811854	NOGENE	EPHX1	chr1	226006283	226006342
A_19_P00803678	NOGENE	EPHX1	chr1	226006301	226006360
A_23_P34537	EPHX1	EPHX1	chr1	226032883	226032942
A_24_P62530	RHOU	RHOU	chr1	228882099	228882158
A_23_P62967	DISC1	TSNAX-DISC1|DISC1	chr1	232176696	232176755
A_33_P3251727	RYR2	RYR2	chr1	237996036	237996095
A_23_P137797	RYR2	RYR2	chr1	237996423	237996482
A_23_P510	PLD5	PLD5	chr1	242252899	242252958
A_32_P8925	C1orf100	C1orf100	chr1	244541935	244552305
A_32_P103291	SMYD3	SMYD3	chr1	245912797	245912856
A_23_P51410	SMYD3	SMYD3	chr1	246490544	246490603
A_19_P00326008	NOGENE	ZNF670-ZNF695	chr1	247126279	247126338
A_19_P00325181	NOGENE	ZNF670-ZNF695	chr1	247138953	247139012
A_19_P00803131	NOGENE	ZNF670-ZNF695	chr1	247142823	247142882
A_23_P35316	ZNF695	ZNF670-ZNF695	chr1	247150712	247150771
A_24_P254705	ZNF695	ZNF670-ZNF695	chr1	247162725	247163255
A_23_P74981	ZNF670	ZNF670-ZNF695|ZNF670	chr1	247200849	247200908
A_23_P86751	ADARB2	ADARB2	chr10	1228144	1228203
A_33_P3282307	ADARB2	ADARB2	chr10	1229183	1229242
A_33_P3282305	ADARB2	ADARB2	chr10	1246262	1246321
A_33_P3244151	NOGENE	ADARB2	chr10	1259513	1259572
A_33_P3416398	LOC100129894	ADARB2	chr10	1334679	1334738
A_33_P3641456	NOGENE	ADARB2	chr10	1379975	1380034
A_24_P206604	PFKFB3	PFKFB3	chr10	6266166	6268203
A_33_P3223663	NOGENE	PFKFB3	chr10	6274345	6274404
A_24_P261259	PFKFB3	PFKFB3	chr10	6277062	6277121
A_33_P3219939	CUBN	CUBN	chr10	16865965	16866024
A_33_P3366758	ST8SIA6	ST8SIA6	chr10	17362676	17362735
A_33_P3403963	ST8SIA6	ST8SIA6	chr10	17363190	17363249
A_23_P161352	PTPLA	PTPLA	chr10	17645575	17645634
A_33_P3235410	PTPLA	PTPLA	chr10	17657511	17657570
A_23_P61580	NSUN6	NSUN6	chr10	18834724	18834783
A_23_P161424	PLXDC2	PLXDC2	chr10	20568719	20568778
A_23_P300905	CCNY	CCNY	chr10	35858729	35858788
A_23_P338495	8-Mar	MARCH8	chr10	45953754	45953813

A_32_P163125	SGMS1	SGMS1	chr10	52065560	52065619
A_33_P3351087	NOGENE	PRKG1	chr10	53822566	53822622
A_24_P250765	PRKG1	PRKG1	chr10	54048737	54050026
A_33_P3258244	PCDH15	PCDH15	chr10	55562664	55562723
A_33_P3258239	PCDH15	PCDH15	chr10	55568452	55568511
A_23_P161331	PCDH15	PCDH15	chr10	55581652	55581711
A_24_P111147	PCDH15	PCDH15	chr10	55754659	55754718
A_33_P3229412	NRG3	NRG3	chr10	84745302	84745361
A_33_P3229417	NRG3	NRG3	chr10	84746874	84746933
A_24_P527404	BMPR1A	BMPR1A	chr10	88683628	88683687
A_23_P1431	BMPR1A	BMPR1A	chr10	88683898	88683957
A_33_P3219256	BMPR1A	BMPR1A	chr10	88684862	88684921
A_33_P3283611	IFIT3	IFIT3	chr10	91099762	91099821
A_23_P500381	HTR7	HTR7	chr10	92500784	92500843
A_33_P3222788	LOC100188947	LOC100188947	chr10	93067061	93067120
A_23_P409489	DNTT	DNTT	chr10	98098081	98098140
A_33_P3220570	UBTD1	UBTD1	chr10	99330900	99330959
A_33_P3293524	NEURL	NEURL	chr10	105352243	105352302
A_23_P202034	GUCY2GP	GUCY2GP	chr10	114074029	114074088
A_24_P882914	C10orf46	C10orf46	chr10	120441482	120441541
A_33_P3377619	C10orf46	C10orf46	chr10	120454654	120454713
A_23_P86599	DMBT1	DMBT1	chr10	124403152	124403211
A_23_P364478	FAM175B	FAM175B	chr10	126524866	126524925
A_23_P87363	ART1	ART1	chr11	3685463	3685523
A_23_P124190	TRIM34	TRIM6-TRIM34|TRIM34	chr11	5655079	5655869
A_24_P398323	TRIM34	TRIM34|TRIM6-TRIM34	chr11	5664680	5664739
A_23_P139418	GALNTL4	GALNTL4	chr11	11292608	11292667
A_23_P150286	PSMA1	PSMA1	chr11	14526569	14526628
A_33_P3288384	PSMA1	PSMA1	chr11	14535512	14535571
A_24_P348806	PLEKHA7	PLEKHA7	chr11	16809231	16809290
A_24_P649282	LUZP2	LUZP2	chr11	25104007	25104066
A_32_P7316	BDNF	BDNF-AS1	chr11	27677013	27677072
A_23_P127891	BDNF	BDNF-AS1	chr11	27679900	27679959
A_33_P3323842	BDNFOS	BDNF-AS1	chr11	27699226	27699285
A_24_P386622	ARRB1	ARRB1	chr11	74977300	74978736
A_23_P162165	KCTD14	NDUFC2-KCTD14	chr11	77727492	77727551
A_23_P363954	THRSP	NDUFC2-KCTD14	chr11	77775305	77775364
A_24_P364236	NDUFC2	NDUFC2-KCTD14|NDUFC2	chr11	77779435	77779494
A_33_P3336652	NDUFC2	NDUFC2-KCTD14|NDUFC2	chr11	77790643	77790702
A_23_P47148	NOX4	NOX4	chr11	89059826	89059885
A_24_P169092	MAML2	MAML2	chr11	95712375	95712434
A_32_P41026	SC5DL	SC5DL	chr11	121183280	121183339
A_32_P158966	KLRF1	KLRF1	chr12	9997324	9997383
A_32_P720220	C12orf36	C12orf36	chr12	13524582	13524641
A_33_P3364089	SLCO1B3	SLCO1B3	chr12	21036476	21036535
A_24_P935986	BCAT1	BCAT1	chr12	24964452	24964511

A_24_P52921	BCAT1	BCAT1	chr12	24989496	24995040
A_23_P95231	CASC1	CASC1	chr12	25261534	25261593
A_33_P3378790	CASC1	CASC1	chr12	25263063	25263122
A_23_P150903	FAR2	FAR2	chr12	29485623	29486586
A_23_P98930	C12orf35	C12orf35	chr12	32145764	32145823
A_33_P3409090	CNTN1	CNTN1	chr12	41352972	41353031
A_23_P390700	CNTN1	CNTN1	chr12	41414156	41414215
A_24_P98914	PFKM	PFKM	chr12	48539724	48539783
A_23_P391443	PPM1H	PPM1H	chr12	63038521	63038580
A_23_P162300	IRAK3	IRAK3	chr12	66642160	66642219
A_23_P113382	GRIP1	GRIP1	chr12	66742133	66742192
A_33_P3252083	GRIP1	GRIP1	chr12	66742800	66742859
A_24_P129834	TPH2	TPH2	chr12	72425334	72425393
A_32_P326819	KRR1	GLIPR1	chr12	75892026	75892085
A_33_P3418125	GLIPR1	GLIPR1	chr12	75895656	75895715
A_33_P3258003	ANKS1B	ANKS1B	chr12	99129338	99129397
A_23_P356717	ANKS1B	ANKS1B	chr12	99138178	99138237
A_33_P3258004	ANKS1B	ANKS1B	chr12	99145177	99145236
A_32_P13113	FAM71C	ANKS1B	chr12	100043693	100043752
A_32_P189204	GAS2L3	GAS2L3	chr12	101018594	101018653
A_33_P3328289	LOC100130902	TXNRD1	chr12	104680606	104680665
A_33_P3328284	NOGENE	TXNRD1	chr12	104680832	104680891
A_23_P65068	EID3	TXNRD1	chr12	104698595	104698654
A_33_P3351120	TXNRD1	TXNRD1	chr12	104732949	104733008
A_23_P348257	NUAK1	NUAK1	chr12	106457546	106457605
A_33_P3371889	NUAK1	NUAK1	chr12	106461077	106461136
A_23_P410312	C12orf76	C12orf76	chr12	110479089	110479148
A_23_P44643	ANAPC7	ANAPC7	chr12	110813991	110815226
A_23_P401361	PITPNM2	PITPNM2	chr12	123468975	123469034
A_33_P3295154	NOGENE	PITPNM2	chr12	123576390	123576449
A_19_P00810888	NOGENE	ZNF664-FAM101A	chr12	124573023	124573082
A_33_P3342862	FAM101A	ZNF664-FAM101A	chr12	124799228	124799287
A_24_P288890	FAM101A	ZNF664-FAM101A	chr12	124799557	124799616
A_23_P308839	TMEM132D	TMEM132D	chr12	129557350	129557409
A_33_P3531979	NOGENE	TMEM132D	chr12	129596347	129596406
A_23_P344037	CHFR	CHFR	chr12	133417712	133417771
A_33_P3327956	ZNF605	ZNF605	chr12	133498048	133498107
A_33_P3352877	SPG20	SPG20	chr13	36875853	36875912
A_33_P3361741	DNAJC15	DNAJC15	chr13	43683245	43683304
A_24_P170774	LRCH1	LRCH1	chr13	47317618	47317677
A_33_P3333337	LRCH1	LRCH1	chr13	47324726	47324785
A_23_P117157	SUCLA2	SUCLA2	chr13	48517388	48517447
A_24_P330263	EDNRB	EDNRB	chr13	78470568	78470627
A_23_P204980	UGGT2	UGGT2	chr13	96453925	96453984
A_23_P205031	COL4A2	COL4A2	chr13	111165261	111165320
A_24_P161973	ATP11A	ATP11A	chr13	113540918	113540977

A_24_P144332	NOGENE	C14orf167	chr14	24408018	24408077
A_32_P118250	C14orf167	C14orf167	chr14	24408338	24408397
A_23_P14351	AKAP6	AKAP6	chr14	33301563	33301622
A_33_P3408420	MDGA2	MDGA2	chr14	47311008	47311067
A_23_P366035	ABHD12B	ABHD12B	chr14	51371212	51371271
A_23_P205623	DDHD1	DDHD1	chr14	53521264	53521323
A_23_P140373	FLVCR2	FLVCR2	chr14	76113756	76113815
A_24_P150486	SPTLC2	SPTLC2	chr14	77973992	77974051
A_24_P42557	TSHR	TSHR	chr14	81557464	81558910
A_23_P88435	FOXN3	FOXN3	chr14	89623539	89623598
A_33_P3363710	LOC100128075	FOXN3	chr14	89734789	89734848
A_24_P306720	LOC400236	FOXN3	chr14	89885621	89885680
A_23_P48771	C14orf159	C14orf159	chr14	91691358	91691417
A_23_P106241	TRIP11	TRIP11	chr14	92435892	92435951
A_33_P3382271	NOGENE	TRIP11	chr14	92506805	92506864
A_23_P432272	KIAA1409	KIAA1409	chr14	94173274	94173333
A_23_P65651	WARS	WARS	chr14	100801041	100801100
A_23_P76731	RAGE	RAGE	chr14	102695289	102695348
A_33_P3326989	RAGE	RAGE	chr14	102698958	102699017
A_33_P3326984	RAGE	RAGE	chr14	102700128	102700187
A_33_P3305958	TECPR2	TECPR2	chr14	102900827	102900886
A_32_P355396	TECPR2	TECPR2	chr14	102968719	102968778
A_33_P3277075	GABRB3	GABRB3	chr15	26788857	26788916
A_33_P3309206	GABRB3	GABRB3	chr15	26869979	26870038
A_23_P129133	OCA2	OCA2	chr15	28000067	28000126
A_32_P143000	FAM189A1	FAM189A1	chr15	29412696	29412755
A_24_P124973	NDNL2	FAM189A1	chr15	29561202	29561261
A_33_P3800734	RYR3	RYR3	chr15	34158044	34158103
A_19_P00328893	NOGENE	LOC729082	chr15	41584871	41584930
A_24_P655268	LOC729082	LOC729082	chr15	41591663	41591722
A_33_P3215277	TTBK2	TTBK2	chr15	43036550	43036609
A_24_P652700	CEP152	CEP152	chr15	49030699	49030758
A_24_P333663	MAPK6	MAPK6	chr15	52356907	52356966
A_23_P3204	MAPK6	MAPK6	chr15	52358055	52358114
A_23_P346006	CCPG1	DYX1C1-CCPG1	chr15	55648436	55648495
A_32_P447001	NOGENE	FLJ27352	chr15	55710662	55710721
A_23_P88559	LIPC	LIPC	chr15	58861011	58861070
A_23_P140475	NOX5	MIR548H4|NOX5	chr15	69348985	69349044
A_19_P00321618	NOGENE	MIR548H4	chr15	69373246	69373305
A_19_P00322896	NOGENE	MIR548H4	chr15	69373297	69373356
A_19_P00319825	NOGENE	MIR548H4	chr15	69373355	69373414
A_19_P00319776	NOGENE	MIR548H4	chr15	69373389	69373448
A_19_P00322671	NOGENE	MIR548H4	chr15	69373449	69373508
A_33_P3214229	TMEM84	MIR548H4	chr15	69373563	69373622
A_19_P00322669	NOGENE	MIR548H4	chr15	69383452	69383511
A_19_P00321910	NOGENE	MIR548H4	chr15	69383675	69383734

A_19_P00322662	NOGENE	MIR548H4	chr15	69387049	69387108
A_23_P322632	TMEM84	MIR548H4	chr15	69387230	69387289
A_19_P00322879	NOGENE	MIR548H4	chr15	69392109	69392168
A_23_P129169	CYP11A1	CYP11A1	chr15	74631018	74631077
A_23_P77304	AP3B2	AP3B2	chr15	83328449	83328642
A_33_P3572454	LOC283692	AP3B2	chr15	83361512	83361571
A_33_P3378081	AGBL1	AGBL1	chr15	87531258	87531317
A_23_P26184	DET1	DET1	chr15	89055798	89055857
A_33_P3229390	NOGENE	DET1	chr15	89061422	89061481
A_24_P287691	AP3S2	C15orf38-AP3S2|AP3S2	chr15	90377719	90377778
A_24_P943017	LASS3	LASS3	chr15	100940872	100940931
A_33_P3408305	LASS3	LASS3	chr15	100942746	100942805
A_24_P48162	MPG	MPG	chr16	133183	133242
A_23_P100326	C16orf35	MPG	chr16	135839	135898
A_33_P3260209	LOC100132944	PMM2	chr16	8941517	8941576
A_23_P432360	PMM2	PMM2	chr16	8942790	8942849
A_23_P140928	TMC7	TMC7	chr16	19074010	19074069
A_23_P420281	PRKCB	PRKCB	chr16	24226173	24226233
A_33_P3294533	PRKCB	PRKCB	chr16	24231495	24231554
A_33_P3255314	FLJ26245	FLJ26245	chr16	34989846	34989905
A_23_P334123	ITFG1	ITFG1	chr16	47192831	47192890
A_33_P3316115	LOC100127930	ITFG1	chr16	47196599	47196658
A_24_P1773	LONP2	LONP2	chr16	48386989	48387048
A_33_P3367293	MT1IP	MT1IP	chr16	56711498	56711557
A_23_P140797	CDH8	CDH8	chr16	61687697	61687756
A_23_P100386	IL34	IL34	chr16	70688562	70690551
A_23_P418234	PHLPP2	PHLPP2	chr16	71679160	71679219
A_33_P3271810	PHLPP2	PHLPP2	chr16	71686698	71686757
A_23_P71972	WWOX	WWOX	chr16	78458922	78466413
A_23_P117992	ATP2C2	ATP2C2	chr16	84497443	84497502
A_33_P3253427	LRRC37B2	LRRC37BP1	chr17	28935520	28935579
A_33_P3564394	SH3GL1P2	LRRC37BP1	chr17	28951611	28951670
A_33_P3564399	SH3GL1P2	LRRC37BP1	chr17	28952259	28952318
A_32_P28402	LRRC37B2	LRRC37BP1	chr17	28964201	28964260
A_23_P389102	MYO1D	MYO1D	chr17	30819832	30819891
A_33_P3399566	LOC100130931	MYO1D	chr17	30903022	30903081
A_24_P119609	MYO1D	MYO1D	chr17	31092008	31092067
A_33_P3221999	GSDMB	GSDMB	chr17	38060850	38060909
A_23_P73150	TTC25	TTC25	chr17	40117524	40117583
A_33_P3289113	COX11	TOM1L1	chr17	53029465	53029524
A_24_P73943	COX11	TOM1L1	chr17	53038703	53038762
A_23_P118493	TOM1L1	TOM1L1	chr17	53038843	53038902
A_23_P375566	STXBP4	STXBP4	chr17	53111534	53111593
A_32_P90483	STXBP4	STXBP4	chr17	53240764	53240823
A_33_P3414362	USP32	USP32	chr17	58329743	58329802
A_24_P410100	NOGENE	USP32	chr17	58356431	58356490

A_19_P00811559	NOGENE	LOC146880	chr17	62758594	62758653
A_23_P66881	RGS9	RGS9	chr17	63223600	63223659
A_23_P84189	PITPNC1	PITPNC1	chr17	65689234	65689293
A_24_P255005	NOGENE	LOC100499466	chr17	66122851	66122910
A_33_P3209404	SH3GL1P3	LOC100499466	chr17	66130414	66130473
A_33_P3314594	RAB37	RAB37	chr17	72742734	72742793
A_23_P414654	RAB37	RAB37	chr17	72743222	72743281
A_23_P38181	GGA3	GGA3	chr17	73232920	73232979
A_23_P26759	CANT1	CANT1	chr17	76988694	76988753
A_24_P116669	CANT1	CANT1	chr17	76993163	76993222
A_23_P327140	RNF213	LOC100294362	chr17	78369857	78369916
A_23_P66948	FAM59A	FAM59A	chr18	29847581	29847640
A_23_P170050	RIT2	RIT2	chr18	40323249	40323308
A_33_P3416588	RIT2	RIT2	chr18	40503555	40503614
A_24_P322354	SKA1	SKA1	chr18	47919899	47919958
A_33_P3401407	hCG_33730	LOC390858	chr18	56718840	56718899
A_33_P3706494	LOC284294	LOC284294	chr18	62090743	62090802
A_33_P3531970	LOC643542	LOC643542	chr18	65566781	65566840
A_23_P101208	CYB5A	CYB5A	chr18	71920718	71920777
A_33_P3311076	CYB5A	CYB5A	chr18	71930598	71930657
A_23_P131074	THEG	THEG	chr19	362125	362184
A_23_P39263	ZNF57	ZNF57	chr19	2917775	2917834
A_23_P360316	FUT3	FUT3	chr19	5843092	5843151
A_23_P101351	ZNF426	ZNF426	chr19	9638979	9639038
A_24_P935782	ZNF121	ZNF121	chr19	9677285	9677344
A_33_P3410925	KLF1	KLF1	chr19	12995236	12995295
A_32_P200238	UCA1	UCA1	chr19	15946035	15946092
A_23_P90419	PBX4	PBX4	chr19	19672538	19672597
A_32_P790361	ZNF90	ZNF90	chr19	20228630	20228689
A_33_P3474538	ZNF90	ZNF90	chr19	20231608	20231667
A_33_P3244574	LOC100128675	LOC100128675	chr19	35550039	35550098
A_23_P406782	HPN	LOC100128675	chr19	35556490	35556549
A_23_P90444	RBM42	RBM42	chr19	36128152	36128211
A_33_P3403773	ZNF569	ZNF569	chr19	37902079	37902138
A_33_P3231602	ZNF569	ZNF569	chr19	37902563	37902622
A_23_P107994	TMEM160	TMEM160	chr19	47549317	47549376
A_23_P368779	ZNF114	ZNF114	chr19	48790154	48790213
A_33_P3327961	ZNF615	ZNF615	chr19	52494748	52494807
A_33_P3400424	ZNF615	ZNF615	chr19	52496133	52496192
A_33_P3345132	ZNF578	ZNF578	chr19	53019319	53019378
A_33_P3256868	ZNF83	ZNF83	chr19	53116271	53116330
A_23_P4962	NLRP5	NLRP5	chr19	56569768	56572812
A_23_P17287	IAH1	IAH1	chr2	9628439	9628498
A_23_P40049	CAD	CAD	chr2	27465770	27465829
A_23_P67847	GALNT14	GALNT14	chr2	31133370	31133429
A_23_P39718	FEZ2	FEZ2	chr2	36779704	36779763

A_33_P3311956	FEZ2	FEZ2	chr2	36782827	36782886
A_33_P3401267	FEZ2	FEZ2	chr2	36787931	36787990
A_33_P3272352	NOGENE	CEBPZ	chr2	37429079	37429138
A_23_P119964	CEBPZ	CEBPZ	chr2	37429942	37430001
A_33_P3223648	NOGENE	CEBPZ	chr2	37430462	37430521
A_33_P3241489	NOGENE	CEBPZ	chr2	37431823	37431882
A_23_P108932	RPL23AP32	SPTBN1	chr2	54756368	54756427
A_33_P3258467	SPTBN1	SPTBN1	chr2	54889385	54889444
A_33_P3258472	SPTBN1	SPTBN1	chr2	54898523	54898582
A_23_P90565	C2orf86	WDPCP	chr2	63486522	63540419
A_23_P253046	UGP2	UGP2	chr2	64118483	64118542
A_23_P56654	MCEE	MCEE	chr2	71337089	71337148
A_23_P5586	MPHOSPH10	MPHOSPH10	chr2	71375141	71375200
A_24_P148590	TACR1	TACR1	chr2	75280843	75347719
A_24_P666105	LRRTM4	LRRTM4	chr2	76974947	76975006
A_33_P3235204	ELMOD3	ELMOD3	chr2	85617562	85617621
A_33_P3297305	ELMOD3	ELMOD3	chr2	85618030	85618089
A_23_P154256	ELMOD3	ELMOD3	chr2	85618691	85618750
A_24_P945293	VPS24	VPS24|RNF103-VPS24	chr2	86730551	86730587
A_24_P240065	VPS24	VPS24|RNF103-VPS24	chr2	86734691	86737514
A_33_P3312489	VWA3B	VWA3B	chr2	98908365	98908424
A_32_P46603	VWA3B	VWA3B	chr2	98920173	98920232
A_23_P373464	AFF3	AFF3	chr2	100163700	100163726
A_23_P108761	C2orf29	C2orf29	chr2	101885805	101885864
A_32_P761797	NCRNA00116	NCRNA00116	chr2	110970211	110970270
A_33_P3402086	NOGENE	MERTK	chr2	112766079	112766138
A_33_P3402091	MERTK	MERTK	chr2	112786885	112786944
A_32_P86578	LOC389023	DPP10	chr2	115901752	115901811
A_33_P3211356	DPP10	DPP10	chr2	116600660	116600719
A_24_P140057	DPP10	DPP10	chr2	116601306	116601365
A_23_P373109	CNTNAP5	CNTNAP5	chr2	125521661	125521720
A_23_P56787	CNTNAP5	CNTNAP5	chr2	125672642	125672701
A_32_P328023	WDR33	WDR33	chr2	128462034	128462093
A_33_P3335840	WDR33	WDR33	chr2	128492971	128493030
A_24_P102920	WDR33	WDR33	chr2	128521179	128521238
A_33_P3335845	WDR33	WDR33	chr2	128522116	128522175
A_33_P3389779	NOGENE	WDR33	chr2	128568324	128568383
A_23_P5342	LRP1B	LRP1B	chr2	140989375	140989434
A_33_P3244728	LRP2	LRP2	chr2	169983769	169983828
A_32_P116857	PDE11A	PDE11A	chr2	178489045	178489104
A_24_P43144	PDE11A	PDE11A	chr2	178545554	178545613
A_33_P3258772	NOGENE	PDE11A	chr2	178587952	178588011
A_33_P3348884	CCDC141	CCDC141	chr2	179698900	179698959
A_33_P3279004	CCDC141	CCDC141	chr2	179700653	179700712
A_33_P3495120	LOC285026	CCDC141	chr2	179737753	179737812
A_19_P00321823	NOGENE	CCDC141	chr2	179783570	179783629

A_19_P00317490	NOGENE	CCDC141	chr2	179791240	179791299
A_19_P00317491	NOGENE	CCDC141	chr2	179791323	179791382
A_19_P00325338	NOGENE	CCDC141	chr2	179815213	179815272
A_19_P00328994	NOGENE	CCDC141	chr2	179828698	179828757
A_19_P00812256	NOGENE	CCDC141	chr2	179866870	179866929
A_19_P00811927	NOGENE	CCDC141	chr2	179866866	179866925
A_19_P00316387	NOGENE	CCDC141	chr2	179914334	179914393
A_32_P316136	ZNF804A	ZNF804A	chr2	185803216	185803275
A_23_P361049	MYO1B	MYO1B	chr2	192289808	192289867
A_23_P363878	RFTN2	RFTN2	chr2	198436064	198436123
A_23_P16817	CLK1	CLK1	chr2	201718707	201719388
A_33_P3211513	CLK1	CLK1	chr2	201725962	201726021
A_33_P3383283	CASP10	CASP10	chr2	202086244	202086303
A_33_P3255075	CASP10	CASP10	chr2	202094051	202094110
A_32_P199462	C2orf80	C2orf80	chr2	209030194	209030253
A_33_P3346966	SPAG16	SPAG16	chr2	215013930	215013989
A_33_P3367984	ABCA12	ABCA12	chr2	215796277	215796336
A_33_P3315134	DIRC3	DIRC3	chr2	218148801	218148860
A_23_P142574	MOGAT1	MOGAT1	chr2	223574531	223574590
A_23_P57110	C20orf54	C20orf54	chr20	741010	741069
A_23_P68511	ANGPT4	ANGPT4	chr20	853663	853722
A_33_P3482534	LOC613266	MACROD2	chr20	15872981	15873038
A_33_P3281033	MACROD2	MACROD2	chr20	15967310	15967369
A_32_P89352	MACROD2	MACROD2	chr20	16033184	16033243
A_23_P6119	SEC23B	SEC23B	chr20	18526643	18529277
A_24_P690924	SEC23B	SEC23B	chr20	18531782	18534900
A_33_P3344046	RP11-218C14.6	CSTT	chr20	23514881	23514940
A_24_P194670	RP11-218C14.6	CSTT	chr20	23514944	23522368
A_33_P3344044	NOGENE	CSTT	chr20	23517548	23517607
A_33_P3359508	DNMT3B	DNMT3B	chr20	31384813	31384872
A_23_P28953	DNMT3B	DNMT3B	chr20	31397064	31397123
A_23_P135576	PTPRT	PTPRT	chr20	40701748	40701807
A_23_P254181	MGC5566	LOC79015	chr20	43285419	43285478
A_23_P120442	NCOA3	NCOA3	chr20	46283630	46283689
A_24_P229536	C21orf34	C21orf34	chr21	17909716	17979329
A_33_P3312384	C21orf34	C21orf34	chr21	17979483	17979542
A_33_P3508822	APP	APP	chr21	27253136	27253195
A_33_P3296479	APP	APP	chr21	27423347	27423406
A_23_P109286	GRIK1	GRIK1	chr21	30927563	30927622
A_33_P3303557	NOGENE	GRIK1	chr21	30968929	30968988
A_23_P413043	C21orf41	GRIK1	chr21	30968994	30969053
A_33_P3279362	NCRNA00110	GRIK1	chr21	31121174	31121233
A_33_P3353471	NCRNA00110	GRIK1-AS1	chr21	31136183	31136242
A_23_P211141	DSCAM	DSCAM	chr21	41384961	41385020
A_23_P154875	BACE2	BACE2	chr21	42647696	42647755
A_33_P3338341	PRODH	PRODH	chr22	18900438	18900497

A_33_P3239295	PRODH	PRODH	chr22	18906965	18907024
A_33_P3239298	NOGENE	PRODH	chr22	18909759	18909818
A_33_P3235335	MTMR3	MTMR3	chr22	30421915	30421974
A_33_P3235330	MTMR3	MTMR3	chr22	30426759	30426818
A_23_P91697	LARGE	LARGE	chr22	33669332	33669391
A_23_P353149	C22orf33	C22orf33	chr22	37387544	37387603
A_33_P3349702	LOC400927	LOC400927	chr22	38740670	38740729
A_33_P3247372	LOC400927	LOC400927	chr22	38755951	38756010
A_33_P3262181	APOBEC3F	APOBEC3F	chr22	39440368	39440427
A_23_P357101	APOBEC3F	APOBEC3F	chr22	39448588	39448647
A_23_P143713	APOBEC3G	APOBEC3G	chr22	39477481	39477540
A_24_P340696	SERHL2	SERHL2	chr22	42968453	42968512
A_23_P120953	SERHL2	SERHL2	chr22	42970262	42970321
A_24_P242036	RRP7B	SERHL2	chr22	42970264	42970323
A_23_P143987	ATG7	ATG7	chr3	11468321	11468380
A_23_P132595	VGLL4	ATG7	chr3	11597959	11598018
A_24_P944827	ATG7	ATG7	chr3	11598763	11598822
A_23_P18282	DLEC1	DLEC1	chr3	38164126	38164185
A_23_P319874	C3orf23	C3orf23	chr3	44400419	44400478
A_23_P373054	C3orf23	C3orf23	chr3	44450680	44450739
A_23_P250302	CCR3	CCR3	chr3	46307828	46307887
A_23_P155463	LRRC2	LRRC2	chr3	46557386	46557445
A_23_P334798	LRRC2	LRRC2	chr3	46563082	46563141
A_33_P3843873	HESRG	ESRG	chr3	54666167	54666226
A_33_P3373259	CACNA2D3	CACNA2D3	chr3	54913050	54913109
A_23_P40856	LRTM1	CACNA2D3	chr3	54958694	54958753
A_24_P402825	CACNA2D3	CACNA2D3	chr3	55021774	55038842
A_32_P14721	DNAH12	DNAH12	chr3	57327797	57327856
A_33_P3216601	FHIT	FHIT	chr3	59737952	59738011
A_33_P3300941	NPCDR1	FHIT	chr3	59957230	59957288
A_33_P3245278	PTPRG	PTPRG	chr3	62280514	62280573
A_23_P80718	SYNPR	SYNPR	chr3	63602485	63602544
A_33_P3253089	FAM19A1	FAM19A1	chr3	68587968	68588027
A_32_P117693	FAM19A1	FAM19A1	chr3	68594375	68594434
A_23_P80503	ROBO1	ROBO1	chr3	78649391	78649450
A_23_P121082	GBE1	GBE1	chr3	81538912	81538971
A_23_P73114	PROS1	PROS1	chr3	93592149	93592208
A_23_P18342	EPHA6	EPHA6	chr3	97367324	97367383
A_33_P3408782	EPHA6	EPHA6	chr3	97467486	97467545
A_23_P212728	TBC1D23	TBC1D23	chr3	100043741	100043800
A_33_P3230319	NOGENE	BBX	chr3	107513790	107513849
A_33_P3369311	BBX	BBX	chr3	107524368	107524427
A_23_P121356	BBX	BBX	chr3	107524534	107524593
A_33_P3301499	C3orf66	C3orf66	chr3	108903960	108904019
A_33_P3358923	BTLA	BTLA	chr3	112182938	112182997
A_23_P212706	ATG3	ATG3	chr3	112255356	112255415

A_23_P92281	GTPBP8	GTPBP8	chr3	112718398	112719742
A_23_P398189	IGSF11	IGSF11	chr3	118619910	118619969
A_23_P166633	ITGB5	ITGB5	chr3	124482491	124482550
A_23_P159316	BFSP2	BFSP2	chr3	133193941	133194001
A_32_P46214	SLC9A9	SLC9A9	chr3	142986095	142986154
A_33_P3313025	NOGENE	SLC9A9	chr3	143346956	143347015
A_23_P40821	HPS3	CP	chr3	148890246	148890304
A_33_P3296587	CP	CP	chr3	148890649	148890708
A_33_P3343196	CP	CP	chr3	148890802	148890861
A_33_P3424297	SELT	SELT	chr3	150344826	150344885
A_33_P3290667	SELT	SELT	chr3	150344862	150344921
A_33_P3305851	SELT	SELT	chr3	150346997	150347056
A_33_P3290672	SELT	SELT	chr3	150348174	150348233
A_33_P3332547	SCHIP1	SCHIP1|IQCJ-SCHIP1	chr3	159606672	159606731
A_32_P62863	SCHIP1	SCHIP1|IQCJ-SCHIP1	chr3	159615048	159615107
A_33_P3214690	NLGN1	NLGN1	chr3	173998992	173999051
A_23_P18123	NLGN1	NLGN1	chr3	174000648	174000707
A_33_P3273854	NAALADL2	NAALADL2	chr3	175523323	175523382
A_24_P85537	MAP3K13	MAP3K13	chr3	185161379	185165590
A_23_P58031	MAP3K13	MAP3K13	chr3	185200168	185200227
A_23_P250156	IGF2BP2	IGF2BP2	chr3	185362047	185362106
A_33_P3242973	IGF2BP2	IGF2BP2	chr3	185363403	185364863
A_33_P3324949	C3orf65	IGF2BP2	chr3	185435895	185435954
A_23_P155939	ZNF595	ZNF718|ZNF595	chr4	86842	86901
A_23_P124438	ZNF718	ZNF718	chr4	156150	156209
A_33_P3274194	KCNIP4	KCNIP4	chr4	20730270	20730329
A_23_P18447	PPARGC1A	PPARGC1A	chr4	23793937	23793996
A_33_P3330952	ATP8A1	ATP8A1	chr4	42410449	42410508
A_23_P81131	CORIN	CORIN	chr4	47596314	47596373
A_23_P110345	CHIC2	CHIC2	chr4	54876232	54876291
A_24_P49687	NOGENE	LPHN3	chr4	62641374	62641433
A_33_P3216746	LPHN3	LPHN3	chr4	62775291	62775350
A_23_P10980	LPHN3	LPHN3	chr4	62937245	62937304
A_33_P3366224	NOGENE	SHROOM3	chr4	77589366	77589425
A_33_P3417328	SHROOM3	SHROOM3	chr4	77637503	77637562
A_33_P3417339	SHROOM3	SHROOM3	chr4	77678028	77678087
A_33_P3336700	SHROOM3	SHROOM3	chr4	77704264	77704323
A_23_P121695	CXCL13	CXCL13	chr4	78532646	78532705
A_23_P110412	TMEM150C	TMEM150C	chr4	83405786	83405845
A_33_P3242231	NOGENE	TMEM150C	chr4	83412519	83412578
A_33_P3851513	LIN54	LIN54	chr4	83846981	83847040
A_33_P3361067	ABCG2	ABCG2	chr4	89011503	89011562
A_33_P3297360	NOGENE	FAM190A	chr4	92240185	92240244
A_32_P306678	FAM190A	FAM190A	chr4	92522638	92522697
A_23_P32847	GRID2	GRID2	chr4	94693252	94693311
A_23_P255376	CCDC109B	CCDC109B	chr4	110605745	110606408

A_23_P7212	CFI	CFI	chr4	110662064	110662123
A_24_P92472	CFI	CFI	chr4	110670656	110670715
A_23_P144458	CAMK2D	CAMK2D	chr4	114381361	114386707
A_33_P3268224	SPATA5	SPATA5	chr4	124240537	124240596
A_33_P3801085	LOC641365	LOC641365	chr4	138948608	138948667
A_33_P3214625	INPP4B	INPP4B	chr4	142949208	142949267
A_33_P3219115	LOC100130178	INPP4B	chr4	143238618	143238677
A_33_P3236436	C4orf51	C4orf51	chr4	146653856	146653915
A_23_P320290	ZNF827	ZNF827	chr4	146686254	146686313
A_33_P3235891	NOGENE	GALNTL6	chr4	173908624	173908683
A_33_P3320017	GALNTL6	GALNTL6	chr4	173961168	173961227
A_33_P3320022	GALNTL6	GALNTL6	chr4	173961500	173961559
A_24_P71904	HPGD	HPGD	chr4	175411686	175411745
A_23_P252236	KLKB1	KLKB1	chr4	187178445	187178504
A_23_P110624	CTNND2	CTNND2	chr5	10973084	10973143
A_19_P00327730	NOGENE	TAG	chr5	12719497	12719556
A_19_P00802660	NOGENE	TAG	chr5	12734994	12735053
A_33_P3826455	TAG	TAG	chr5	12759692	12759751
A_33_P3265941	NOGENE	TAG	chr5	12794242	12794301
A_19_P00316231	NOGENE	TAG	chr5	12804384	12804443
A_24_P7600	FBXL7	FBXL7	chr5	15937236	15937295
A_23_P144827	FBXL7	FBXL7	chr5	15939565	15939624
A_32_P10936	CDH12	CDH12	chr5	21751312	21751368
A_23_P92727	RAI14	RAI14	chr5	34831952	34832011
A_24_P40795	NOGENE	NNT	chr5	43667002	43667061
A_23_P70148	NNT	NNT	chr5	43704546	43704605
A_33_P3365995	MAST4	MAST4	chr5	66255013	66255072
A_23_P110571	MAST4	MAST4	chr5	66462808	66462867
A_23_P259521	WDR41	WDR41	chr5	76728963	76729022
A_33_P3359846	NOGENE	SERINC5	chr5	79439878	79439937
A_23_P423457	SERINC5	SERINC5	chr5	79473159	79473218
A_24_P111912	FAM172A	FAM172A	chr5	92953936	92953995
A_23_P358564	POU5F2	FAM172A	chr5	93076020	93076079
A_33_P3401058	NOGENE	FAM172A	chr5	93198654	93198713
A_24_P149124	C5orf13	C5orf13	chr5	111065091	111065150
A_33_P3391290	C5orf13	C5orf13	chr5	111066368	111066427
A_23_P346982	DTWD2	DTWD2	chr5	118175647	118175706
A_23_P144999	RAPGEF6	RAPGEF6	chr5	130762075	130762134
A_33_P3243519	RAPGEF6	RAPGEF6	chr5	130766553	130766612
A_33_P3243524	RAPGEF6	RAPGEF6	chr5	130771644	130771703
A_23_P110643	CDKL3	CDKL3	chr5	133643886	133643945
A_33_P3337632	TRPC7	TRPC7	chr5	135549123	135549182
A_24_P140569	LRRTM2	CTNNA1	chr5	138205569	138205628
A_33_P3251024	LRRTM2	CTNNA1	chr5	138208699	138208758
A_33_P3403418	CTNNA1	CTNNA1	chr5	138266534	138266593
A_23_P58647	CTNNA1	CTNNA1	chr5	138270387	138270446

A_32_P222695	FLJ41603	ARHGEF37	chr5	149014156	149014215
A_33_P3245218	ODZ2	ODZ2	chr5	167689754	167689813
A_24_P299474	ODZ2	ODZ2	chr5	167690063	167690122
A_23_P58819	RANBP17	RANBP17	chr5	170725916	170725975
A_23_P321307	ADAMTS2	ADAMTS2	chr5	178608104	178634520
A_33_P3411204	GCNT2	GCNT2	chr6	10627251	10627310
A_24_P397489	GCNT2	GCNT2	chr6	10628471	10628530
A_24_P277657	GMPR	GMPR	chr6	16290766	16290825
A_33_P3212109	DCDC2	DCDC2	chr6	24172180	24172239
A_24_P166407	HIST1H4B	HIST1H4B	chr6	26027149	26027208
A_23_P259098	ZSCAN16	ZSCAN16	chr6	28097263	28097322
A_23_P42288	C6orf27	C6orf27	chr6	31734142	31734279
A_33_P3342420	NOGENE	DNAH8	chr6	38899007	38899066
A_23_P145159	DNAH8	DNAH8	chr6	38980339	38980398
A_23_P145175	ZNF318	ZNF318	chr6	43303992	43304051
A_24_P204043	ZNF318	ZNF318	chr6	43316128	43316187
A_24_P204144	NOGENE	ZNF318	chr6	43331750	43331810
A_23_P402187	PKHD1	PKHD1	chr6	51480343	51480402
A_23_P424617	PKHD1	PKHD1	chr6	51586468	51586527
A_33_P3387420	PKHD1	PKHD1	chr6	51524767	51609241
A_32_P480330	EYS	EYS	chr6	64430448	64430507
A_33_P3276833	EYS	EYS	chr6	64430609	64430668
A_19_P00803113	NOGENE	EYS	chr6	64472319	64472378
A_33_P3276808	NOGENE	EYS	chr6	64472322	64472381
A_19_P00321801	NOGENE	EYS	chr6	64472463	64472522
A_19_P00321802	NOGENE	EYS	chr6	64487899	64487958
A_19_P00316319	NOGENE	EYS	chr6	64488013	64488072
A_19_P00321803	NOGENE	EYS	chr6	64488009	64488068
A_33_P3276818	EYS	EYS	chr6	65303024	65303083
A_33_P3276828	NOGENE	EYS	chr6	65532725	65532784
A_33_P3276813	EYS	EYS	chr6	65596591	65596650
A_33_P3276805	NOGENE	EYS	chr6	66005651	66005710
A_24_P944973	EYS	EYS	chr6	66044872	66044931
A_33_P3359115	LMBRD1	LMBRD1	chr6	70385779	70385838
A_33_P3248799	TRDN	TRDN	chr6	123869600	123869659
A_23_P93524	SAMD3	SAMD3	chr6	130465781	130465840
A_23_P397937	SAMD3	SAMD3	chr6	130505674	130505733
A_23_P134113	C6orf192	C6orf192	chr6	133090550	133090609
A_33_P3321230	C6orf192	C6orf192	chr6	133095381	133095440
A_23_P134125	MAP3K5	MAP3K5	chr6	136878349	136878408
A_33_P3377130	MAP3K5	MAP3K5	chr6	136901467	136901526
A_33_P3246580	KIAA1244	KIAA1244	chr6	138657434	138657493
A_23_P393880	KIAA1244	KIAA1244	chr6	138659313	138659372
A_33_P3387951	KIAA1244	KIAA1244	chr6	138662672	138662731
A_33_P3416574	AIG1	AIG1	chr6	143458067	143458126
A_33_P3416563	AIG1	AIG1	chr6	143654522	143654581

A_23_P93431	AIG1	AIG1	chr6	143661259	143661318
A_33_P3412087	C6orf97	C6orf97	chr6	151939801	151939860
A_33_P3270489	C6orf97	C6orf97	chr6	151942097	151942156
A_23_P500861	SYNE1	SYNE1	chr6	152443052	152443111
A_33_P3335920	SYNE1	SYNE1	chr6	152443528	152443587
A_33_P3288919	NOGENE	SYNE1	chr6	152488859	152488918
A_33_P3335915	SYNE1	SYNE1	chr6	152748771	152748830
A_33_P3335910	SYNE1	SYNE1	chr6	152757076	152757134
A_24_P58308	NOGENE	ARID1B	chr6	157298027	157298086
A_33_P3291877	ARID1B	ARID1B	chr6	157469939	157469998
A_33_P3291882	NOGENE	ARID1B	chr6	157507679	157507738
A_23_P70701	ARID1B	ARID1B	chr6	157529022	157529081
A_33_P3333078	NOGENE	ARID1B	chr6	157531787	157531846
A_23_P382045	TULP4	TULP4	chr6	158932662	158932721
A_33_P3312119	LOC100130967	C6orf99	chr6	159331223	159331282
A_23_P111395	SLC22A2	SLC22A2	chr6	160638226	160638285
A_23_P136077	PARK2	PARK2	chr6	161769778	161769837
A_23_P145134	FGFR1OP	FGFR1OP	chr6	167453724	167453783
A_32_P415151	WDR27	WDR27	chr6	170033151	170034569
A_23_P336992	ZFAND2A	ZFAND2A	chr7	1195219	1197349
A_33_P3251227	C1GALT1	C1GALT1	chr7	7278507	7278566
A_23_P252145	C1GALT1	C1GALT1	chr7	7283565	7283624
A_19_P00805702	NOGENE	C1GALT1	chr7	7288141	7288200
A_24_P129277	NOD1	NOD1	chr7	30464987	30465046
A_24_P272967	AVL9	AVL9	chr7	32598953	32599012
A_23_P122947	AVL9	AVL9	chr7	32619842	32620430
A_23_P145718	AOAH	AOAH	chr7	36561708	36570069
A_23_P319027	HECW1	HECW1	chr7	43602391	43602450
A_23_P45087	ZNF107	ZNF107	chr7	64171177	64171236
A_23_P111517	WBSCR17	WBSCR17	chr7	71177978	71178037
A_23_P215484	CCL26	CCL26	chr7	75399061	75401219
A_23_P416894	PION	PION	chr7	76940387	76940446
A_33_P3280694	PION	PION	chr7	76958871	76958930
A_23_P21376	MAGI2	MAGI2	chr7	77646565	77646624
A_33_P3311992	MAGI2	MAGI2	chr7	77649075	77649134
A_33_P3312802	RPL13AP17	MAGI2	chr7	77988714	77988773
A_24_P123833	SEMA3E	SEMA3E	chr7	82993805	82993864
A_23_P59528	ACN9	ACN9	chr7	96810787	96810846
A_23_P358917	CYP3A7	CYP3A7	chr7	99303037	99303096
A_33_P3318117	CYP3A7	CYP3A7	chr7	99303139	99303198
A_33_P3264404	LOC100132593	CUX1	chr7	101818665	101818724
A_33_P3298785	CUX1	CUX1	chr7	101892263	101892322
A_24_P220454	CUX1	CUX1	chr7	101893025	101893084
A_23_P253375	CUX1	CUX1	chr7	101926989	101927048
A_23_P59637	DOCK4	DOCK4	chr7	111366266	111366325
A_33_P3253420	NOGENE	DOCK4	chr7	111611353	111611412

A_33_P3354001	CADPS2	CADPS2	chr7	121958491	121958550
A_23_P42963	RNF133	CADPS2	chr7	122338036	122338095
A_24_P170234	RNF148	CADPS2	chr7	122341976	122342035
A_33_P3397418	ZC3HAV1	ZC3HAV1	chr7	138728351	138728410
A_33_P3298980	NOGENE	ZC3HAV1	chr7	138734016	138734075
A_23_P20122	ZC3HAV1	ZC3HAV1	chr7	138745443	138745502
A_33_P3251801	KLRG2	KLRG2	chr7	139138088	139138147
A_33_P3306207	KLRG2	KLRG2	chr7	139138858	139138917
A_23_P309224	AGK	AGK	chr7	141353184	141353243
A_33_P3367196	CNTNAP2	CNTNAP2	chr7	148117937	148117996
A_33_P3264089	ACTR3C	ACTR3C	chr7	149992342	149992401
A_24_P132383	GIMAP8	GIMAP8	chr7	150175990	150176049
A_33_P3230244	CSMD1	CSMD1	chr8	2792900	2792959
A_33_P3230249	CSMD1	CSMD1	chr8	2984937	2984996
A_23_P31798	NAT2	NAT2	chr8	18258142	18258201
A_23_P94103	SCARA5	SCARA5	chr8	27727875	27727934
A_23_P215931	LEPROTL1	LEPROTL1	chr8	29965452	29965511
A_24_P306824	MBOAT4	LEPROTL1	chr8	29989463	29989522
A_33_P3252206	LEPROTL1	LEPROTL1	chr8	29995141	29995200
A_23_P72527	ADAM18	ADAM18	chr8	39581412	39587461
A_23_P83835	SGK196	SGK196	chr8	42977869	42977928
A_24_P4170	CPA6	CPA6	chr8	68396078	68396957
A_33_P3391778	RALYL	RALYL	chr8	85441725	85441784
A_33_P3316899	RALYL	RALYL	chr8	85799861	85799920
A_23_P388220	RALYL	RALYL	chr8	85799966	85833142
A_23_P371861	CNBD1	CNBD1	chr8	88298829	88298888
A_23_P252106	RIPK2	RIPK2	chr8	90802345	90802404
A_33_P3371219	SDC2	SDC2	chr8	97623978	97624037
A_24_P180680	LAPTM4B	LAPTM4B	chr8	98864581	98864640
A_24_P332816	RIMS2	RIMS2	chr8	104928692	104928751
A_23_P147786	RIMS2	RIMS2	chr8	105263899	105263958
A_24_P106794	NUDCD1	NUDCD1	chr8	110253382	110253441
A_23_P60166	DEPDC6	DEPTOR	chr8	121062582	121062641
A_19_P00321436	NOGENE	HHLA1	chr8	133073733	133073792
A_33_P3301050	HHLA1	HHLA1	chr8	133073733	133073792
A_19_P00319204	NOGENE	HHLA1	chr8	133076177	133076236
A_19_P00330652	NOGENE	HHLA1	chr8	133088841	133088900
A_19_P00321196	NOGENE	HHLA1	chr8	133090100	133090159
A_19_P00319586	NOGENE	HHLA1	chr8	133092154	133092213
A_23_P384023	GLIS3	GLIS3	chr9	3828374	3829334
A_33_P3326568	GLIS3	GLIS3	chr9	3855481	3855540
A_23_P312837	C9orf70	GLIS3	chr9	3898837	3898896
A_33_P3309551	PTPRD	PTPRD	chr9	8314275	8314334
A_24_P639665	NOGENE	PTPRD	chr9	8861154	8861213
A_32_P395879	C9orf93	C9orf93	chr9	15920369	15971614
A_33_P3608210	LOC554202	LOC554202	chr9	21454716	21454775

A_23_P302060	IFNE	LOC554202	chr9	21481102	21481161
A_24_P255100	C9orf135	C9orf135	chr9	72471488	72471547
A_23_P32078	SLC28A3	SLC28A3	chr9	86900326	86900385
A_23_P43326	SPTLC1	SPTLC1	chr9	94793717	94793776
A_32_P48949	C9orf129	C9orf129	chr9	96080485	96080544
A_33_P3351175	WNK2	C9orf129	chr9	96082754	96082813
A_23_P157970	INVS	INVS	chr9	103062898	103062957
A_24_P235429	ABCA1	ABCA1	chr9	107543704	107543763
A_33_P3422897	ABCA1	ABCA1	chr9	107624012	107624071
A_23_P411806	SLC44A1	SLC44A1	chr9	108136938	108136997
A_23_P216630	SLC44A1	SLC44A1	chr9	108153508	108153567
A_23_P146486	1-Dec	DEC1	chr9	118164718	118164777
A_23_P216894	MAPKAP1	MAPKAP1	chr9	128200564	128200623
A_33_P3251538	MAPKAP1	MAPKAP1	chr9	128305339	128305398
A_33_P3397755	MAPKAP1	MAPKAP1	chr9	128347923	128347982
A_33_P3407937	PLCXD1	PLCXD1	chrX	208260	208319
A_23_P61180	PLCXD1	PLCXD1	chrX	219727	219786
A_23_P217704	GYG2	GYG2	chrX	2800115	2800174
A_23_P254842	HDHD1A	HDHD1	chrX	6967361	6967420
A_23_P429950	KAL1	KAL1	chrX	8497233	8497292
A_24_P940275	FRMPD4	FRMPD4	chrX	12739959	12740018
A_24_P672240	FRMPD4	FRMPD4	chrX	12742371	12742430
A_33_P3780311	LOC349408	LOC349408	chrX	12921157	12921216
A_23_P73837	TLR8	LOC349408	chrX	12940262	12940321
A_33_P3224595	OFD1	OFD1	chrX	13769427	13769486
A_24_P134653	OFD1	OFD1	chrX	13786879	13787218
A_33_P3394178	NHS	NHS	chrX	17750175	17750234
A_32_P126375	NHS	NHS	chrX	17753480	17753539
A_33_P3351510	IL1RAPL1	IL1RAPL1	chrX	29973954	29974013
A_24_P185854	DMD	DMD	chrX	31137349	31137408
A_33_P3284763	DMD	DMD	chrX	31152220	31152279
A_23_P321860	DMD	DMD	chrX	31196312	31196342
A_33_P3297818	NOGENE	DMD	chrX	31199562	31199621
A_24_P195724	NOGENE	DMD	chrX	32224776	32224837
A_33_P3297813	DMD	DMD	chrX	32535057	32535116
A_33_P3297808	NOGENE	DMD	chrX	32562406	32562465
A_33_P3415087	CLCN5	CLCN5	chrX	49856988	49857047
A_33_P3415092	CLCN5	CLCN5	chrX	49863833	49863892
A_23_P113471	FAAH2	FAAH2	chrX	57515446	57515505
A_24_P404840	GJB1	BCYRN1	chrX	70444287	70444346
A_23_P137073	ZMYM3	BCYRN1	chrX	70459456	70459485
A_24_P16815	ZMYM3	BCYRN1	chrX	70469422	70469481
A_33_P3247753	TSIX	TSIX	chrX	73027005	73027064
A_33_P3341686	XIST	TSIX	chrX	73040506	73040565
A_19_P00331623	NOGENE	TSIX	chrX	73040566	73040625
A_19_P00329511	NOGENE	TSIX	chrX	73040688	73040747

A_19_P00323692	NOGENE	TSIX	chrX	73040697	73040756
A_19_P00319151	NOGENE	TSIX	chrX	73040732	73040791
A_19_P00321129	NOGENE	TSIX	chrX	73041907	73041966
A_19_P00321917	NOGENE	TSIX	chrX	73043015	73043074
A_19_P00802872	NOGENE	TSIX	chrX	73043696	73043755
A_19_P00806762	NOGENE	TSIX	chrX	73043894	73043953
A_19_P00332515	NOGENE	TSIX	chrX	73047086	73047145
A_19_P00320438	NOGENE	TSIX	chrX	73048929	73048988
A_19_P00316565	NOGENE	TSIX	chrX	73049001	73049060
A_19_P00326132	NOGENE	TSIX	chrX	73049003	73049062
A_33_P3405911	TSIX	TSIX	chrX	73049007	73049066
A_19_P00319561	NOGENE	MIR374AHG	chrX	73289101	73289160
A_19_P00320488	NOGENE	MIR374AHG	chrX	73289534	73289593
A_33_P3294985	NCRNA00183	MIR374AHG	chrX	73289703	73289762
A_19_P00318107	NOGENE	MIR374AHG	chrX	73290680	73290739
A_33_P3407235	LOC100133180	MIR374AHG	chrX	73351716	73351775
A_32_P464135	DACH2	DACH2	chrX	86087385	86087444
A_33_P3363465	NOGENE	PCDH11X	chrX	91355188	91355247
A_33_P3346448	PCDH11X	PCDH11X	chrX	91873836	91873895
A_23_P254212	RPA4	DIAPH2	chrX	96140272	96140331
A_23_P85004	DIAPH2	DIAPH2	chrX	96369895	96369954
A_24_P144303	LOC442459	LOC442459	chrX	98716600	98716642
A_33_P3318424	NOGENE	BHLHB9	chrX	102000979	102001038
A_23_P308954	BHLHB9	BHLHB9	chrX	102006979	102007038
A_33_P3319176	HTR2C	HTR2C	chrX	114143005	114143064
A_23_P433586	HTR2C	HTR2C	chrX	114143855	114143914
A_33_P3281308	LOC286467	LOC286467	chrX	130836687	130836746
A_19_P00325063	NOGENE	LOC286467	chrX	130845660	130845719
A_32_P137980	PCDH11Y	PCDH11Y	chrY	5610107	5610166
A_23_P160017	TTTY11	TTTY11	chrY	8652207	8657062

Table S1D. List of primer sequences

	Figures			sequence	others
pyro sequencing	Fig.1F	hPON3	forward primer	GGGAATGGAGGGGAGTTTTAGTTTAGAG	cg24750391
			reverse primer	CCTATCTTTTCCTTCTTTTCTCCTAATAT (5'-biotinylated)	
			sequence primer	TGTTTTATTTAGGAGTGTGTTG	
	Fig. 1G	hTCERG1L	forward primer	GGGTGTTTGGTTTGAAGTT (5'-biotinylated)	cg03943081
			reverse primer	AATAATCCTACCCCACCCAAAAAATATC	
			sequence primer	CCACCTACCTAATACCTT	
	Fig. 3F	hABHD12B 5'LTR-1	forward primer	TGTGTATTAATGTATGGTTAATTTTGGTAA	
			reverse primer	CAAACCATCTAAACAAATACCTACAA (5'biotinylated)	
			sequence primer	GTTGTTTTTTATGTAGTGTTT	
		hABHD12B 5'LTR-2	forward primer	TGTGTATTAATGTATGGTTAATTTTGGTAA	
			reverse primer	CAAACCATCTAAACAAATACCTACAA (5'biotinylated)	
			sequence primer	TTAGGTTTTTGAGTTTAAGTTAA	
		hABHD12B	forward primer	AAGTTTGTTTGGTGGTTTTTTTATATAGA (5'biotinylated)	

		3'LTR	reverse primer	ACCATTCCACAATCATAATAAAATACTTT	
			sequence primer	ACCAATAACAATAAACAAAATTT	
		hHHLA1 3'LTR	forward primer	AAAGTTTGTTTGGTGGTTTTTT	
			reverse primer	AAAAAAATTAATCTCCTCCATATACCTT (5'biotinylated)	
			sequence primer	TTGTTTGGTGGTTTTTTTA	
		hC4orf51 5'LTR	forward primer	GGATAATTTGAAAATGTTTTTGGTTAAGG	
			reverse primer	ATAATTCTTCAATTACTTCAAACCATCTA (5'biotinylated)	
			sequence primer	GGTTTTTGAGTTTAAGTTAAG	
		hC4orf51 3'LTR	forward primer	TTTTTTTTTTGGTTTATTTTGGTTTAAAAG	
			reverse primer	ACAAACCATATCTCAAATAAAAAATTTCAT (5'biotinylated)	
			sequence primer	ATATAAAATTTGTTTGGTGG	
	Fig. S1C	hA2BP1	forward primer	TAAGA TGAAA AGTGG AAAGA AATAG	Doi et al., (ref)
			reverse primer	ATAAA AACTC TAAAC CCAAC CATCA (5'biotinylated)	
			sequence primer	GAAGA TTTTA TAGTT ATTTT AAATA G	
		hIGF1R	forward primer	AAGGT TTTTT ATTTG TTTTT GATTA	Doi et al., (ref)
			reverse primer	AAAAT CCTAA ACCCT CCACT TC (5'biotinylated)	
			sequence primer	AGGTT TTTTA TTTGT TTTTG ATTA	
		hPOU3F4	forward primer	ATTTT TGTGT GTATG TGTTT TTGTG	Doi et al., (ref)
			reverse primer	CTCTA CACAA CCTAA CCAAA TTTTT (5'biotinylated)	
			sequence primer	ATTTT TGTGT GTATG TGTTT TTGTG	
		hPTPRT	forward primer	GAGAT TAGTG ATGGA ATATT TTTGA TTTTG (5'biotinylated)	Doi et al., (ref) modified
			reverse primer	ACCCC AAACA ATCCT AAAAA TCCAA ACAT	
			sequence primer	AACTCA AATTT TATAT CCTCT	
		hZNF184	forward primer	TTGGG AGAGT TTTAA AGTTA TTTGG	Doi et al., (ref)
			reverse primer	TAACT CCAAT CCAAA ATTTT CTCTC (5'biotinylated)	
			sequence primer	TGGGA GAGTT TTAAA GTTAT TTGGA	
	Fig. S3C	ARRB1 LTR	forward primer	TGTTGGGATTATAGGGGTGA	
			reverse primer	ACAAACCATTTTCACTTCTTTTATCAT (5'-biotinylated)	
			sequence primer	GAGTTTAAGTTAAGATATTATAGTT	
		FAAH2 LTR	forward primer	AAAGTTTGTTTGGTGGTTTTTT (5'-biotinylated)	
			reverse primer	AAATACCCTCTCTCACTACTCTAATAC	
			sequence primer	ACTTCAACAAAATCTCAATT	
		TBC1D23 LTR	forward primer	AAAGTTTGTTTGGTGGTTTTTT (5'-biotinylated)	
			reverse primer	CCACACATAACTTAAAACTAACATATTAAT	
			sequence primer	ACCTCTAAATAAAATAACTTTCA	
bisulfite clonal sequencing	Fig. S3C	DNMT3B LTR	1st forward primer	AGAAGAAAAAAGTAAGTTTATAAAGGTATT	
			1st reverse primer	ACCACCAACCTTTCTTTACCTTAATCCT	
			2nd forward primer	ATGTATTGTTAGGTTTTTGAGTTTAAG	
			2nd reverse primer	CTCCCAAACATAAATCAAATACCA	
		ABCA1 LTR	1st forward primer	GGGAAATTTAAAATTAAGGTGTTGG	
			1st reverse primer	CCCCCCTCAAAATTCATACAT	
			2nd forward primer	AGGTTTTTAAGTTTAAGTTAAGT	
			2nd reverse primer	CACAAATACCATAAATTTCATAT	
		APP LTR	1st forward primer	AGTAT TTTAT AGTTA TATGT TGT	
			1st reverse primer	TATTT CTTTA CCCAC ATCTT CTT	
			2nd forward primer	TGTTG TGATA ATAAA GAGAT TTT	

			2nd reverse primer	TATTT CTTTA CCCAC ATCTT CTT	
qPCR	Fig. 4E	total OCT3/4	forward primer	CCCCAGGGCCCCATTTTGGTACC	
			reverse primer	ACCTCAGTTTGAATGCATGGGAGAGC	
	Fig. 4F	SOX17	forward primer	CGCTTTCATGGTGTGGGCTAAGGACG	
			reverse primer	TAGTTGGGGTGGTCCTGCATGTGCTG	
	Fig. 4G	GOOSECOID	forward primer	GAGGAGAAAGTGGAGGTCTG	
			reverse primer	CTCTGATGAGGACCGCTTCTG	
	Fig. S2A	hPAX6	forward primer	ACCCATTATCCAGATGTGTTTGCC CGA G	
			reverse primer	ATGGTGAAGCTGGGCATAGGCGGCAG	
		hMAP2	forward primer	CAGGTGGCGGACGTGTGAAAATTGAGAGTG	
			reverse primer	CACGCTGGATCTGCCTGGGGACTGTG	
	Fig. S5C	total KLF4	forward primer	CATGCCAGAGGAGCCCAAGCCAAAGAGGGG	
			reverse primer	CGCAGGTGTGCCTTGAGATGGGAACTCTTT	
		retroviral Tg KLF4	forward primer	CCACCTCGCCTTACACATGAAGA	
			reverse primer	GACATGGCCTGCCCGGTTATTATT	
	Fig. S5D	total OCT3/4	forward primer	CCC CAG GGC CCC ATT TTG GTA CC	
			reverse primer	ACCTCAGTTTGAATGCATGGGAGAGC	
		retroviral Tg OCT3/4	forward primer	GCTCTCCCATGCATTCAAACTGA	
			reverse primer	CTTACGCGAAATACGGGCAGACA	

Table S2. Information about transplantation, graft size and compoments

	experiment No.	clone name	passage No.	qPCR (pre-transplantation)	Graft size (Day30)	Graft size (Day60)	graft		
							neural	non-neural	
defective (42)	#0	TKCBV5-6	p99	N.D.	N.D.	N.D.	0	10	A
	#1-1	TKCBV5-6	p101	✓	N.D.	8.552	1	9	A
	#1-2	TKCBV5-6	p101	✓	N.D.	9.66	2	8	A
	#3-1	TKCBV5-6	p82	✓	4.939	10.15	9	1	D
	#3-2	TKCBV5-6	p82	✓	4.787	16.46	6	4	B
	#3-3	TKCBV5-6	p82	✓	8.556	20.68	8	2	C
	#0	TIG118-4f1	p43	N.D.	N.D.	20.35	9	1	D
	#1-1	TIG118-4f1	p45	✓	N.D.	4.888	10	0	E
	#1-2	TIG118-4f1	p45	✓	N.D.	38.71	8	2	C
	#3-1	TIG118-4f1	p53	✓	1.056	22.66	3	7	A
	#3-2	TIG118-4f1	p53	✓	3.492	16.62	8	2	C
	#3-3	TIG118-4f1	p53	✓	9.194	28.85	9	1	D
	#0	TIG108-4f3	p36	N.D.	N.D.	N.D.	7	3	C
	#1-1	TIG108-4f3	p30	✓	N.D.	Died	5	5	B
	#1-2	TIG108-4f3	p30	✓	N.D.	Died	5	5	B
	#3-1	TIG108-4f3	p17	✓	10.86	Died	6	4	B
	#3-3	TIG108-4f3	p17	✓	17.88	Died	5	5	B
	#4-1	TIG108-4f3	p18	✓	6.601	Died	5	5	B
	#4-2	TIG108-4f3	p18	✓	6.889	16.71	6	4	B
	#4-3	TIG108-4f3	p18	✓	14.82	Died	7	3	C
	#9-1	1503-4f1-1	p54	✓	3.152	12.87	9	1	D
	#9-1	1503-4f1-2	p54	✓	0.783	12.328			N.D.
	#0	TIG107-3f1	p48	N.D.	N.D.	N.D.	5	5	B
	#1-1	TIG107-3f1	p56	✓	N.D.	Died	7	3	C
	#1-2	TIG107-3f1	p56	✓	N.D.	Died	5	5	B
	#2-1	TIG107-3f1	p56	✓	21.05	Died	9	1	D
	#2-2	TIG107-3f1	p56	✓	11.03	Died	9	1	D
	#2-3	TIG107-3f1	p56	✓	21.25	Died	9	1	D
	#0	451F3	p75	N.D.	N.D.	22.81	9	1	D
	#1-1	451F3	p77	✓	N.D.	11.43	10	0	E
	#1-2	451F3	p77	✓	N.D.	13.14	10	0	E
	#2-1	451F3	p65	✓	2.61	7.556	10	0	E
	#2-2	451F3	p65	✓	2.937	9.967	8	2	C
	#2-3	451F3	p65	✓	8.2	34.77	7	3	C
	#7-1	451F3	p63	✓	4.852	11.82	10	0	E
	#7-2	451F3	p63	✓	2.441	6.26	9	1	D
	#7-3	451F3	p63	✓	2.99	1.46	1	9	A

neural tissue containing	
0-4	A
5-6	B
7-8	C
9	D
10	E
not determined	N.D.

	#2-1	TIG107-4f1	p24	✓	3.608	14.17	6	4	B
	#2-2	TIG107-4f1	p24	✓	3.801	23.31	7	3	C
	#2-3	TIG107-4f1	p24	✓	4.889	24.22	6	4	B
	#9-1	TIG107-4f1-1	p24	✓	2.076	12.07	5	5	B
	#9-1	TIG107-4f1-2	p24	✓	3.715	10.598	6	4	B
intermediate (9)	#8-2	604A1	p32	✓	N.D.	N.D.			N.D.
	#8-3	604A1	p32	✓	2.411	7.894	10	0	E
	#8-1	610B1	p24	✓	1.196	4.279	10	0	E
	#8-2	610B1	p24	✓	1.906	3.741	10	0	E
	#8-3	610B1	p24	✓	0.7776	1.968	10	0	E
	#0	khES1	p79	N.D.	N.D.	12.32	10	0	E
	#7-1	khES1	p72	✓	4.879	9.16	10	0	E
	#7-2	khES1	p72	✓	4.65	8.917	10	0	E
	#7-3	khES1	p72	✓	2.66	6.951	8	2	C
good (63)	#8-1	604B1	p24	✓	2.924	5.083	10	0	E
	#8-2	604B1	p24	✓	2.131	5.082	10	0	E
	#8-3	604B1	p24	✓	1.852	8.705	10	0	E
	#7-1	TKCBV4-2	p77	✓	0.862	9.654	0	10	A
	#7-2	TKCBV4-2	p77	✓	0.193	Died	0	10	A
	#7-3	TKCBV4-2	p77	✓	1.992	6.908	0	10	A
	#7-1	TKCB7-2	p41	✓	2.751	12.776	10	0	E
	#7-2	TKCB7-2	p41	✓	1.666	2.939	10	0	E
	#7-3	TKCB7-2	p41	✓	0.76	Died	6	4	B
	#0	H9	p47	N.D.	N.D.	N.D.	10	0	E
	#2-1	H9	p50	✓	1.338	3.081	10	0	E
	#2-2	H9	p50	✓	N.D.	N.D.	10	0	E
	#2-3	H9	p50	✓	4.403	13.42	10	0	E
	#4-1	H9	p16	✓	3.047	10.49	9	1	D
	#4-2	H9	p16	✓	5.178	15.91	9	1	D
	#4-3	H9	p16	✓	1.625	5.94	5	5	B
	#7-1	606A1	p27	✓	2.359	2.903	10	0	E
	#7-2	606A1	p27	✓	N.D.	5.734	10	0	E
	#7-3	606A1	p27	✓	5.241	16.14	10	0	E
	#8-2	606B1	p23	✓	2.184	6.033	10	0	E
	#8-3	606B1	p23	✓	1.655	1.646	10	0	E
	#3-1	253G4	p27	✓	1.19	1.814	10	0	E
	#3-2	253G4	p27	✓	0.5012	1.252	10	0	E
	#3-3	253G4	p27	✓	1.219	1.839	10	0	E
	#2-1	201B7	p25	✓	0.8161	1.747	10	0	E
	#2-2	201B7	p25	✓	1.462	2.485	10	0	E
	#2-3	201B7	p25	✓	2.052	2.568	10	0	E
	#0	khES3	p76	N.D.	N.D.	2.405	10	0	E
	#1-1	khES3	p78	✓	N.D.	1.177	10	0	E

	#1-2	khES3	p78	✓	N.D.	0.5812	10	0	E
	#3-1	khES3	p76	✓	1.105	6.036	10	0	E
	#3-3	khES3	p76	✓	1.321	2.151	10	0	E
	#8-2	604A3	p25	✓	2.528	4.077	10	0	E
	#8-3	604A3	p25	✓	1.611	2.911	10	0	E
	#7-1	409B2	p24	✓	0.5389	1.034	10	0	E
	#7-2	409B2	p24	✓	0.541	1.093	10	0	E
	#7-3	409B2	p24	✓	0.627	0.2324	10	0	E
	#8-1	H1	p56	✓	2.652	9.702	10	0	E
	#8-2	H1	p56	✓	3.089	8.957	10	0	E
	#8-3	H1	p56	✓	2.124	23.46	9	1	D
	#9-1	H1-1	p62	✓	2.954	8.729	10	0	E
	#9-1	H1-2	p62	✓	2.367	13.34			N.D.
	#7-1	585A1	p24	✓	2.627	5.63	9	1	D
	#7-2	585A1	p24	✓	4.3	17.33	9	1	D
	#7-3	585A1	p24	✓	3.623	5.309	6	4	B
	#8-1	585A1	p25	✓	4.18	9.747	10	0	E
	#8-2	585A1	p25	✓	2.07	6.665	10	0	E
	#8-3	585A1	p25	✓	2.562	6.714	10	0	E
	#7-1	414C2	p23	✓	1.03	2.919	10	0	E
	#7-2	414C2	p23	✓	1.21	2.441	10	0	E
	#7-3	414C2	p23	✓	1.229	2.498			N.D.
	#2-1	253G1	p25	✓	0.8773	3.505	10	0	E
	#2-2	253G1	p25	✓	0.9547	1.308	10	0	E
	#2-3	253G1	p25	✓	3.066	4.442	10	0	E
	#8-1	610A2	p25	✓	1.47	3.751	10	0	E
	#8-2	610A2	p25	✓	1.963	3.279	10	0	E
	#8-3	610A2	p25	✓	2.143	3.452	10	0	E
	#7-1	454E2	p23	✓	3.126	N.D.	9	1	D
	#7-2	454E2	p23	✓	1.241	4.443	1	9	A
	#7-3	454E2	p23	✓	1.051	2.35	1	9	A
	#3-1	201B6	p26	✓	0.7227	1.992	10	0	E
	#3-2	201B6	p26	✓	0.5638	1.034	10	0	E
	#3-3	201B6	p26	✓	0.3843	Died			N.D.
control	#8-1	medium			0	0			
	#8-2	medium			0	0			
	#8-3	medium			0	0			
	#9-1	PBS			0	0			

Dataset S1. Information of hESCs/hiPSCs used in this study

	Clone Name	Cell type	Method	Source				Factors (**)	reference	initial feeder	SNL-culture started	molecular signatues		Differentiation	SFEBq experiment					
				Origin	Age (y)	Sex	Race (*)					gene & miRNA expression	methylation	Teratoma	karyotype (***)		SFEBq passage No.	OCT3/4 (%) after SFEBq	Number of trials	mRNA/miRNA
1	KhES1	ES		blastocyst		F			Suemori et al., 2006	MEF&SL10	p16-	✓ (p30)	✓ (p30)	✓	Not checked	intermediate	p21,p24,p24,p27,p25,p26,p26,p27,p72	0,0.8,0.08,0.13,0.07,0.01,1.7,0.59,0.00	9	✓ (p26)
2	KhES3	ES		blastocyst		M			Suemori et al., 2006	MEF&SL10	p20-	✓ (p37)	✓ (p37)	✓	✓46,XY [30] (p36)	good	p73	0.2	1	✓ (p61)
3	KhES4	ES		blastocyst		M			Suemori et al., unpublished	MEF&SL10	p36-	✓ (p44)	✓ (p44)		Not checked	good	p46,p48,p51	0.13,0.45,0.06	3	✓ (p49)
4	KhES5	ES		blastocyst		M			Suemori et al., unpublished	MEF&SL10	p34-	✓ (p47)	✓ (p47)		Not checked	good	p50,p42,p45	0.22,0.02,0	3	✓ (p43)
5	H1	ES		blastocyst		M			from WiCell, Thomson et al., 1998	MEF	p31-	✓ (p49)	✓ (p49)	✓	✓47,XY,+12[3]/47,XY,+mar[20](p78)	good	p56,p62	0.13, 0.09	2	✓ (p57)
6	H9	ES		blastocyst		F			from WiCell, Thomson et al., 1998	MEF	p26-	✓ (p40)	✓ (p40)	✓	✓46,XX [20] (p65)	good	p40,p45,p45,p38,p39,p48	0,0.05,0.1,0.05,0,0.3	6	✓ (p47)
7	ES03	ES		blastocyst		F			from WiCell	MEF	p58-	✓ (p65)	✓ (p60)		Not checked	good	p72,p75,p78	0.12,0.04,0.03	3	✓ (p76)
8	ES04	ES		blastocyst		M			from WiCell	MEF	p57-	✓ (p74)	✓ (p63)		Not checked	good	p81,p89,p92	0.33,0.1,0.28	3	✓ (p90)
9	ES06	ES		blastocyst		F			from WiCell	MEF	p36-	✓ (p43)	✓ (p41)		Not checked	good	p50,p53,p56	0.17,0.05,0.04	3	✓ (p54)
10	SA02	ES		blastocyst		F			from WiCell	MEF	p27-	✓ (p32)	✓ (p32)		Not checked	good	p33,p36	0,0.02	2	✓ (p34)
11	201B2	iPS	Retrovirus	Fibro (HDF1388)	36	F	C	OSKM	Takahashi et al., 2007	SNL	iPS induction	✓ (p67)	✓ (p67)	✓	✓47,XX,+12 [20] (p22)	good	p73,p74	0.05,0.4	2	✓ (p79)
12	201B6	iPS	Retrovirus	Fibro (HDF1388)	36	F	C	OSKM	Takahashi et al., 2007	SNL	iPS induction	✓ (p25)	✓ (p25)	✓	✓46,XX [50] (p10)	good	p23,p24	0.03,0.02	2	✓ (p17)
13	201B7	iPS	Retrovirus	Fibro (HDF1388)	36	F	C	OSKM	Takahashi et al., 2007	SNL	iPS induction	✓ (p18)	✓ (p18)	✓	✓46,XX [20] (p22)	good	p20,p23,p18,p19,p21,p22,p29	0.15,0.26,0,0.0,0.01, 0.04	7	✓ (p22)
14	253G1	iPS	Retrovirus	Fibro (HDF1388)	36	F	C	OSK	Takahashi et al., 2007	SNL	iPS induction	✓ (p32)	✓ (p32)	✓	✓a (p21)	good	p27,p28,p29	0,0,0.1	3	✓ (p22)
15	253G4	iPS	Retrovirus	Fibro (HDF1388)	36	F	C	OSK	Takahashi et al., 2007	SNL	iPS induction	✓ (p30)	✓ (p30)	✓	✓46,XX [20] (p15)	good	p20,p21	0.28,0.1	2	✓ (p21)
16	TIG103-4f4	iPS	Retrovirus	Fibro (TIG103)	69	F	J	OSKM	Takahashi et al., unpublished	SNL	iPS induction	✓ (p8)	✓ (p8)							
17	TIG107-4f1	iPS	Retrovirus	Fibro (TIG107)	81	F	J	OSKM	Amps et al., 2011	SNL	iPS induction	✓ (p18)	✓ (p21)	✓	✓46,XX [50] (p13)	defective	p17,p21,p24	0.92,3.62,11.20	3	✓ (p24)
18	TIG107-3f1	iPS	Retrovirus	Fibro (TIG107)	81	F	J	OSK	Amps et al., 2011	SNL	iPS induction	✓ (p57)	✓ (p57)	✓	✓47,XX,+12[20] (p55)	defective	p25,p26,p29,p24	0,7.64,14.25,1.19	4	✓ (p31)
19	TIG108-4f3	iPS	Retrovirus	Fibro (TIG108)	40	F	J	OSK(M)	Takahashi et al., unpublished	SNL	iPS induction	✓ (p16)	✓ (p19)	✓	✓46,XX [20] (p20)	defective	p18,p22,p21,p22,p19,p20,p19	1.24,12.41,8.4,8.9,14.9,14.16,4.0	7	✓ (p24)
20	TIG109-4f1	iPS	Retrovirus	Fibro (TIG109)	39	F	J	OSKM	Takahashi et al., unpublished	SNL	iPS induction	✓ (p20)	✓ (p21)							
21	TIG114-4f1	iPS	Retrovirus	Fibro (TIG114)	36	M	J	OSKM	Amps et al., 2011	SNL	iPS induction	✓ (p21)	✓ (p21)		✓b (p14)	good	p13,p17	0.04,0.04	2	✓ (p15)
22	TIG118-4f1	iPS	Retrovirus	Fibro (TIG118)	12	F	J	OSKM	Takahashi et al., unpublished	SNL	iPS induction	✓ (p10)	✓ (p10)	✓	✓46,XX,add(7)(q11.2)[20] (p19)	defective	p14,p18,p17,p13,p15,p16	17.47,5.19,12.6,8.3,6.94,17.1	6	✓ (p20)
23	TIG120-4f1	iPS	Retrovirus	Fibro (TIG120)	6	F	J	OSKM	Amps et al., 2011	SNL	iPS induction	✓ (p16)	✓ (p21)	✓	✓46,XX [50] (p16)	intermediate	p17,p20	0,3.64	2	✓ (p23)
24	TIG121-4f4	iPS	Retrovirus	Fibro (TIG121)	8 month	M	J	OSKM	Takahashi et al., unpublished	SNL	iPS induction	✓ (p16)	✓ (p28)							
25	1375-4f1	iPS	Retrovirus	Fibro (HDF1375)	41	F	C	OSKM	Takahashi et al., unpublished	SNL	iPS induction	✓ (p10)	✓ (p10)		Not checked	good	p18,p21	0.01,0.07	2	✓ (p24)
26	1377-4f1	iPS	Retrovirus	Fibro (HDF1377)	53	F	C	OSKM	Takahashi et al., unpublished	SNL	iPS induction	✓ (p13)	✓ (p13)							
27	1392-4f2	iPS	Retrovirus	Fibro (HDF1392)	56	M	C	OSKM	Takahashi et al., unpublished	SNL	iPS induction	✓ (p19)	✓ (p19)							
28	1488-4f1	iPS	Retrovirus	Fibro (HDF1488)	50	F	C	OSKM	Takahashi et al., unpublished	SNL	iPS induction	✓ (p27)	✓ (p20)	✓	Not checked	good	p22,p25	0,0.09	2	✓ (p27)
29	1503-4f1	iPS	Retrovirus	Fibro (HDF1503)	73	F	C	OSKM	Takahashi et al., unpublished	SNL	iPS induction	✓ (p28)	✓ (p28)		✓ 46,XX [20] (p40)	defective	p46,p45,p54	1.11, 13.06,14.39	3	✓ (p38)
30	1687-4f2	iPS	Retrovirus	Fibro (HDF1687)	34	F	C	OSKM	Takahashi et al., unpublished	SNL	iPS induction	✓ (p12)	✓ (p12)							
31	DP31-4f1	iPS	Retrovirus	DP31	14	F	J	OSKM	Tamaoki et al., 2010	SNL	iPS induction	✓ (p13)	✓ (p10)	✓						
32	225C7	iPS	Retrovirus	Fibro (HDF1419)	22 weeks	F	unknown	OSKM	Takahashi et al., unpublished	SNL	iPS induction	✓ (p14)	✓ (p14)							
33	246G1	iPS	Retrovirus	BJ	neonatal	M	unknown	OSKM	Takahashi et al., 2007	SNL	iPS induction	✓ (p15)	✓ (p15)	✓	✓46,XY[20] (p23)	good	p17,p21	0,0.05	2	✓ (p23)
34	TKCBV4-2	iPS	Retrovirus	CB CD34$^+$/CD45$^+$	0	M	unknown	OSKM	Kajiwara et al., 2012	MEF	p45-	✓ (p82)	✓ (p74)		✓46,XY[20] (p82)	good	p75,p80,p77	0,0.35,0.49	3	✓ (p82)
35	TKCBV5-6	iPS	Retrovirus	CB CD34$^+$/CD45$^+$	0	M	unknown	OSKM	Kajiwara et al., 2012	MEF	p45-	✓ (p73)	✓ (p72)	✓	✓46,XY[20] (p75)	defective	p67,p71,p71,p72,p76,p77	10.74,8.69,19.01,9.6,14.44,12.78	6	✓ (p73)
36	TKCB7-2	iPS	Retrovirus	CB CD34$^+$/CD45$^+$	0	M	unknown	OSKM	Kajiwara et al., 2012	MEF	p12-	✓ (p42)	✓ (p38)		✓c (p42)	good	p33,p38,p41	0,0.39,0.04	3	✓ (p42)
37	404C2	iPS	Episomal plasmid	Fibro (HDF1388)	36	F	C	OSKUL+shp53	Okita et al., 2011	MEF	p1-	✓ (p44)	✓ (p48)	✓	✓d (p44)	good	p39,p44	0,0.02	2	✓ (p44)
38	409B2	iPS	Episomal plasmid	Fibro (HDF1388)	36	F	C	OSKUL+shp53	Okita et al., 2011	MEF	p1-	✓ (p52)	✓ (p45)	✓	✓46,XX[20] (p48)	good	p44,p24	0.16,0.02	2	✓ (p48)
39	414C2	iPS	Episomal plasmid	Fibro (HDF1388)	36	F	C	OSKUL+shp53	Okita et al., 2011	MEF	p1-	✓ (p55)	✓ (p55)	✓	✓46,XX[20] (p52)	good	p44,p48,p23	0.11,0.05,0.10	3	✓ (p52)
40	451F3	iPS	Episomal plasmid	DP74	16	F	J	OSKUL+shp53	Okita et al., 2011	SNL	iPS induction	✓ (p41)	✓ (p40)	✓	✓46,XX[20] (p43)	defective	p36,p39,p38,p39,p44,p45,p63	13.61,13.91,2.42,6.1,2.18,1.3,1.96	7	✓ (p41)
41	454E2	iPS	Episomal plasmid	DP74	16	F	J	OSKUL+shp53	Okita et al., 2011	SNL	iPS induction	✓ (p46)	✓ (p48)	✓	✓46,XX[20] (p45)	good	p37,p41,p23	0.01,0.06,0.08	3	✓ (p46)
42	585A1	iPS	Episomal plasmid	PBMN αβT (donor x)	30s	M	J	OSKUL+shp53	Kajiwara et al., 2012	MEF	p1-	✓ (p16)	✓ (p16)	✓	✓46,XY[20] (p15)	good	p18,p24,p25	0.1,0.04,0.13	3	✓ (p16)
43	585B1	iPS	Episomal plasmid	PBMN αβT (donor x)	30s	M	J	OSKUL+shp53	Kajiwara et al., 2012	MEF	p1-	✓ (p16)	✓ (p16)	✓						
44	604A1	iPS	Episomal plasmid	PBMN αβT (donor y)	30s	M	J	OSKUL+shp53	Kajiwara et al., 2012	MEF	p1-	✓ (p14)	✓ (p14)	✓	✓46,XY[20] (p13)	intermediate	p16,p32	4.7,0.02	2	✓ (p14)
45	604A3	iPS	Episomal plasmid	PBMN αβT (donor y)	30s	M	J	OSKUL+shp53	Kajiwara et al., 2012	MEF	p1-	✓ (p14)	✓ (p14)	✓	✓46,XY[20] (p13)	good	p17,p25	0.2,0.02	2	✓ (p14)
46	604B1	iPS	Episomal plasmid	PBMN αβT (donor y)	30s	M	J	OSKUL+shp53	Kajiwara et al., 2012	MEF	p1-	✓ (p13)	✓ (p13)	✓	✓46,XY[20] (p12)	good	p16,p24	0.1,0.94	2	✓ (p13)
47	606A1	iPS	Episomal plasmid	CB CD34$^+$ (donor a)	0	F	unknown	OSKUL+shp53	Kajiwara et al., 2012	MEF	p1-	✓ (p14)	✓ (p14)	✓	✓46,XX[20] (p13)	good	p17,p27	0.3,0.01	2	✓ (p14)
48	606B1	iPS	Episomal plasmid	CB CD34$^+$ (donor a)	0	F	unknown	OSKUL+shp53	Kajiwara et al., 2012	MEF	p1-	✓ (p13)	✓ (p13)	✓	✓46,XX[20] (p12)	good	p16,p23	0.3,0.07	2	✓ (p13)
49	610A2	iPS	Episomal plasmid	CB CD34$^+$ (donor b)	0	M	unknown	OSKUL+shp53	Kajiwara et al., 2012	MEF	p1-	✓ (p14)	✓ (p14)	✓	✓e (p13)	good	p17,p25	0.1,0.03	2	✓ (p14)
50	610B1	iPS	Episomal plasmid	CB CD34$^+$ (donor b)	0	M	unknown	OSKUL+shp53	Kajiwara et al., 2012	SNL	iPS induction	✓ (p14)	✓ (p14)	✓	✓46,XY[20] (p13)	intermediate	p17,p24	4.7,0.10	2	✓ (p14)
51	622E1	iPS	Sendai virus	PBMN αβT (donor y)	30s	M	J	OSKM	Kajiwara et al., 2012	MEF	p1-	✓ (p18)	✓ (p18)	✓	✓46,XY[20] (p15)	good	p18,p25	0.1,0.1	2	✓ (p18)
52	622G1	iPS	Sendai virus	PBMN αβT (donor y)	30s	M	J	OSKM	Kajiwara et al., 2012	MEF	p1-	✓ (p19)	✓ (p19)	✓	✓46,XY[20] (p16)	good	p19,p26	0.1,0.2	2	✓ (p19)
53	703A1	iPS	Sendai virus	PBMN αβT (donor x)	30s	M	J	OSKM	Kajiwara et al., 2012	MEF	p1-	✓ (p17)	✓ (p17)	✓	✓46,XY[20] (p14)	intermediate	p17,p22,p24	0.1,1.3,1.3	3	✓ (p17)
54	703B1	iPS	Sendai virus	PBMN αβT (donor x)	30s	M	J	OSKM	Kajiwara et al., 2012	MEF	p1-	✓ (p17)	✓ (p17)	✓	✓46,XY[20] (p13)	good	p17,p21,p24	0.1,0.2,0.4	3	✓ (p17)
55	665A1	iPS	Sendai virus	CB CD34$^+$ (donor b)	0	M	unknown	OSKM	Kajiwara et al., 2012	MEF	p1-	✓ (p17)	✓ (p16)	✓	✓46,XY[20] (p14)	good	p17,p21,p24	0.9,0.7,0.7	3	✓ (p17)
56	665A7	iPS	Sendai virus	CB CD34$^+$ (donor b)	0	M	unknown	OSKM	Kajiwara et al., 2012	MEF	p1-	✓ (p18)	✓ (p16)	✓	✓46,XY[20] (p15)	good	p18,p21,p25	0,0.1,0.1	3	✓ (p18)
57	711A1	iPS	Sendai virus	CB CD34$^+$ (donor a)	0	F	unknown	OSKM	Okita et al., unpublished	MEF	p1-	✓ (p12)	✓ (p12)		✓f (p22)	good	p12,p18	0.3,0.1	2	✓ (p12)
58	711A6	iPS	Sendai virus	CB CD34$^+$ (donor a)	0	F	unknown	OSKM	Okita et al., unpublished	MEF	p1-	✓ (p13)	✓ (p13)	✓	✓46,XX[20] (p10)	good	p13,p19	0.2,0.3	2	✓ (p13)
59	711C1	iPS	Sendai virus	CB CD34$^+$ (donor a)	0	F	unknown	OSKM	Okita et al., unpublished	MEF	p1-	✓ (p14)	✓ (p14)	✓	✓46,XX[20] (p10)	good	p14,p20	0.1,0	2	✓ (p14)

(*) C: Caucasian, J: Japanese

(**) O: OCT3/4, S: SOX2, K: KLF4, M: C-MYC, U: L-MYC, L: LIN28, shp53: shRNA of p53

(***) (a) 46,XX[19], 45,XX,-1,+5,-6,-11,-12,+20,+20[1], (b) 46,XY[49], 48,XY, del(9)(q11), +2mar [1], (c) 46,XY[18], 47,XY,+12[1], 47,XY,+Y,-9,+12[1], (d) 47,XX,add(7)(q32),add(8)(p21),+12[13], 46,XX,add(8)(p23)[6], 46,XX[1], (e) 46,XY[19] 46,XY,-1,add(18)(p11.2),der(19)t(1;19)(q21;p13.1),+mar[1], (f) 46,X,-Xor-Y,add(18)(q?21),+mar [20]